Chair of Transportation Systems Engineering
Departement of Civil, Geo and Environmental Engineering
Technical University of Munich

Parameter Calibration and Stochastic Model Extension for an Agent-Based Simulation of Vertiport Ground Operations

A thesis presented in part fulfilment of the requirements of the Degree of Master of Science in Transportation Systems at the Department of Civil, Geo and Environmental Engineering, Technical University of Munich.

Supervised by	Dr. Raoul Rothfeld M.Sc. Lukas Preis Chair of Transportation Systems Engineering
Submitted by	Susan Cheng Arcisstrasse 21 80333 München
Submitted on	München, 31.10.2021

Abstract

Urban Air Mobility (UAM) introduces a mode of fast transport that can potentially help travelers escape congestion in major metropolitans worldwide. Due to the emergence of electric propulsion as a key technological driver, UAM has become an increasingly relevant topic in transportation over the past several years. Although technology for electric Vertical Takeoff and Landing (eVTOL) vehicles has advanced significantly, literature reveals that vertiport infrastructure and operation have not been adequately developed and can become critical bottlenecks in the realization of UAM. To increase the understanding of vertiport infrastructure, this thesis aims to extend an existing agent-based vertiport simulation model by calibrating operational parameters through expert interviews and expanding the model through stochastic extensions of input parameters. The expert interviews include 17 participants from relevant industries and academia who estimated expected values, minimum values, maximum values, and confidence levels for selected parameters. A final parameter list of 24 deterministic values is calibrated using weighted averaging of 53 datapoints from literature and 63 responses from experts. Furthermore, these expert responses are modeled by aggregating individual skew normal distributions into normal distributions and further prepared through Monte Carlo simulations as input parameters for the vertiport simulation. Various deterministic and stochastic scenarios were simulated to shed light on the sensitivities of vertiport operations. Results reveal three main conclusions: firstly, the calibration of deterministic parameters produces behavioral differences in operations, which both verifies and produces insight to the simulation. Secondly, stochastic variation in passenger and vehicle behaviors produces negligible differences, inferring that stochastic variation of agent behavior is unnecessary. Lastly, results demonstrate that stochastic distribution of arrival and departure times in the simulation produces measurable impact on the results.

Acknowledgments

Thank you all who have supported me throughout the duration of this thesis. To my supervisor, M.Sc. Lukas Preis, thank you for not only being a supervisor to me but also a friend. It was a privilege to work with you and receive your patient guidance throughout my work.

To my TUM supervisor, Dr. Raoul Rothfeld, thank you for your highly interesting lectures in emerging mobility technologies which initially captured my interest in the field of Urban Air Mobility.

Finally, thank you to my family and friends for always supporting me with encouraging words and prayer.

Table of Contents

List of Figures

List of Tables

1. Introduction

Urbanization is on the rise today, with more than half of the world's population living in cities and a noticeable trend of people moving into urban areas. In mid-2021, 4.5 out of 7.9 billion people, or 57% of the world population, lived in cities, and this number is expected to rise to 60% by 2030 [10]. With growing cities, the development of good transportation becomes inevitable as congestion creates inescapable issues that ripple into all areas of society. Mobility becomes a high-priority topic as the main catalyst of urban symbiosis and stability. In an age of automation, technology, and connectivity, there is much interest and investment in advances of future mobility such as electric and shared mobility [11]. Furthermore, individual travel is highly promoted and emerging mobility service providers race to serve urban dwellers the fastest and cheapest inner-city travel. With such a landscape as the driver to many highly technological achievements, the evolution of smart transportation takes the stage for cutting-edge scientific research and market development today.

As ridesharing and pooling become increasingly prevalent today, the topic of urban mobility and transport is also growing in popularity. Efficient transportation is a critical factor in every developing city and long commute time often poses as a major concern in congested metropolitans. According to Uber Elevate's market study in 2016, "on-demand aviation, has the potential to radically improve urban mobility, giving people back time lost in their daily commutes" [12]. Therefore, the term "Urban Air Mobility" (UAM), referring to air transportation of passenger or cargo in urban environments, was created and became a high-priority topic in urban transport. In 2020, the Federal Aviation Administration (FAA) developed its first UAM Concept of Operations (ConOps), describing it as "the envisioned operational environment that supports the expected growth of flight operations in and around urban areas" [13]. With the attention focused on air traffic operations in urban settings, UAM is a subset of Advanced Air Mobility (AAM), an air transportation system serving passengers and cargo across both urban and rural skies. UAM seeks to support the transition from traditional passenger flights in international settings to passenger and cargo flights in urban settings. In addition to experts from renowned aerospace institutions, individual researchers from various disciplines also provide extensive examination into UAM. An exemplary proposal by Preis seeks to create a top layer for UAM systems by using text mining to identify the top seven associated fields as: air traffic management, infrastructure, market, operator, passenger, public, and vehicle [14]. Structural approaches as such create a reference point from which parties of interest can springboard into further discussions regarding UAM development.

A closer look into the viability of UAM identifies infrastructure as a critical factor in actualizing UAM operations. A market study from Deloitte attributes the biggest hurdle for future air mobility to the design and implementation of required ground infrastructure [15]. For the urban setting, vertiplaces—infrastructure with takeoff and landing pads—would require necessary operational procedures to handle passenger processing and vehicle movements. Obvious options for vertiplaces include existing airports, helipads, and open land expanses; alternatives under consideration are vertiports, which are situated in the heart of cities (e.g. building tops). The Booz Allen Hamilton market study comments that although infrastructure constraints are a significant barrier to UAM, it could be addressed through development and expansion of vertiports [16]. Since the context of the study is the urban landscape, the focus of the author's research is vertiports, on which vehicles arrive and depart by Vertical Takeoff and Landing (VTOL). Specifically, the author investigates and discusses parameters relevant for vertiport ground operations in order to provide a relevant, realistic framework for future vertiport developers. This is conducted through expert interviews and stochastic modeling, both of which will be expounded later in the thesis.

1.1 Motivation

Though interest for helicopter taxis is on the rise, research around vertiport and ground operations are lacking in literature. There is a potential to use existing helicopter and airplane infrastructure; however, operations specific to vertical takeoff and landing vehicles require further study and investigation in a UAM context before related actions (i.e. legislation, construction) can be realized. The author's personal motivation for selecting this topic is to address and conquer the challenges of using urban skies as a novel means of transport by focusing on vertiport infrastructure. Through this study, the author hopes to contribute to the development of UAM into a robust form of transportation while ensuring security, reliability, and efficiency.

1.2 Objective

This thesis seeks to answer the following questions: what are the critical designs and processes that occur on a vertiport, and how can these processes be parametrized and quantified? The author specifically defines the critical drivers for vertiport operations and parameters that represent realistic vertiport ground operations. Furthermore, the parameter study, deterministic modeling, and stochastic modeling are active approaches that will be used to further calibrate the input parameters for the agent-based vertiport simulation developed by Preis [8]. The effects of the calibrated parameters on vertiport simulation outputs will also be discussed and analyzed to determine the validity of the mathematical models.

1.3 Thesis outline

The rest of the thesis is structured as follows:

Chapter 2 describes the state-of-the-art regarding vertiport ground operations, including the existing vertiport framework simulation that serves as the primary model for parameter definition and study.

Chapter 3 discusses the methods used to conduct scientific expert interviews, determine critical parameters, and stochastically model expert responses into normal distributions.

Chapter 4 presents the results of the expert interviews, final list of critical vertiport parameters, deterministic and stochastic models, and the vertiport simulation outputs. These outputs include: 1) one scenario with the deterministic model using default parameter inputs, 2) one scenario with the deterministic model using calibrated parameter values, and 3) threes scenario with the stochastic model using values from the newly-derived stochastic curves as parameter inputs.

Chapter 5 consists of a discussion of the comparison between the five aforementioned simulation runs and an interpretation of results.

Chapter 6 delineates the work done in this study and introduces limitations and recommendations of future work that can further the present study.

2. State-of-the-art

This chapter summarizes the development of urban air mobility, the achievements regarding vertiports in the scientific community, and identifies the research gaps in the field.

2.1. Urban air mobility (UAM)

NASA defines urban air mobility as “safe and efficient air traffic operations in a metropolitan area for manned aircraft and unmanned aircraft systems” [17]. UAM is also described by the FAA as a transportation system that “will use highly automated aircraft that will operate and transport passengers or cargo at lower altitudes within urban and suburban areas” [18]. It seeks to be incorporated in multi-modal city transportation and efficiently transport people by means of shorter distances and travel time. In a study of potential time savings UAM can provide, it is estimated that UAM can reduce travel time for 3% to 13% of shared motorized trips that are beyond the distances of a 50-55 minute car ride [19]. Along with the introduction of UAM comes the numerous considerations of safety, security, governmental regulations, airspace compatibility, and community acceptance. UAM also explores electrification as the primary means of vehicle energy while taking a deeper look into vehicle automation. In urban driving, it is found that a 30% to 95% overall reduction of carbon emissions was obtained through electrification and that electric vehicles transfer CO2 emissions from the transportation sector to the electric sector [20]. In terms of automation, NASA’s market study on UAM focuses on two likely cases where automation will be applied to urban air transport: air metro and air taxi [21]. Air metro will serve to autonomously operate public transit services in the air, while the air taxi will be an autonomous, ride-sharing vehicle accessible on-demand. Although not necessary criterion for UAM, vehicle autonomy and electrification are highly considered in the development of urban air transport.

2.2. Existing eVTOL market competitors

There are 68 companies today producing winged electric Vertical Takeoff and Landing (eVTOL) vehicles and 16 companies producing wingless eVTOLs in the race for mass realization of urban air mobility [22]. Some outstanding prototypes belong to the companies Lilium, Aurora LightningStrike, and Joby Aviation. These vectored-thrust eVTOLs use wings to cruise efficiently and use a propulsion system for both hover and cruise abilities [23]. According to the same reference, other winged aircrafts such as the Aurora

Flight Sciences, Kitty Hawk Cora, and ZeeAero Z-P2 have two separate propulsion systems for hover and cruise flight [23]. Furthermore, the most advanced wingless eVTOLs include the E-Hang 184 and Volocopter 2X, multirotors that specialize in short distance flights and can sustain hover through large disk actuator surfaces. These eVTOLs are best used in inner-city, short-range operations to escape ground congestion and increase travel time savings. After building working prototypes, the next step for eVTOL companies is to test their vehicles and obtain flight certification for their aircrafts. The leaders in eVTOL certification are EHang EH216, Volocopter's VoloCity, Joby Aviation S4, and Lilium [24]. Additionally, EHang, a Chinese company, has been testing their aircrafts since 2018 and submitted their certification application in 2020 in hopes of being certified by the end of 2022 [24]. Volocopter, a German manufacturer, is the first eVTOL manufacturer to obtain European Union Aviation Safety Agency (EASA) approval for their two-seater design and aims for the EASA SC-VTOL (special condition VTOL) certification by the end of 2022. Another German start-up, Lilium, built seven-seater aircrafts that will undergo testing in 2022 and begin commercial flights in 2024 and network operations in 2025. Joby Aviation, a US-based company, can accommodate four seats and aim to obtain its certification from the Federal Aviation Administration (FAA) by 2022 and begin urban operations in 2024. eVTOL manufacturers realize that working with novel technology calls for working "parallel," indicating that training and operation must proceed simultaneously with the certification process [25]. Novel technology also requires unique compliances, which must be clearly communicated by eVTOL manufacturers to certification regulators to obtain user acceptance.

Figure 1: Lilium Jet (above) and Volocopter (below). Source: [1], [2].

2.3. On-demand services

Modern helicopter operators provide services through an on-demand, ride-sharing model. In this study, vertiport operations will be simulated to operate like on-demand, ride-sharing services. Booked like conventional airplane rides, these services are easily accessible by customers through online or mobile bookings. However, recent helicopter services also operate in similar fashion to ground taxis – rides can be booked on-demand. In 2014, BLADE founded its air charter broker and indirect carrier service and offers helicopter flights between New York, Miami, and Aspen while investing in projects that will begin to “transition existing routes to eVTOL aircraft starting in 2025” [26]. Then, in 2016, Airbus’s Voom was the first to launch a mobile helicopter booking platform and initiate operations in Brazil, Mexico, and the US [27]. Although its services ceased in the midst of the COVID-19 pandemic, Voom’s next goal is to “democratize access to urban skies,” having gained approximately 150,000 users in its four years of operation. Uber, the most popular on-demand ride-hailing service worldwide, cooperated with direct air carrier HeliFlite in 2019 to service trips between Manhatten and JFK International Airport [28]. Known as the “Uber Copter,” Uber provides flights with options for customers be picked up or dropped off in selected heliports within a defined location, or travel door-to-door. Requests are to be booked directly through the Uber app just like normal taxi rides. Uber’s next step towards UAM involves its decision to be purchased by Joby Aviation, a company developing eVTOLs for air taxi services in late 2020 [29]. This acquisition would allow the integration of Joby’s air travel services with Uber’s ground transport through Uber’s ride-hailing app.

Figure 2: Uber partners with Joby. Source: [3].

2.4. Vertical takeoff and landing vehicles (eVTOLs)

Vertical takeoff and landing vehicles are designed to hover, takeoff, and land vertically. Their distinguishing trait from conventional aircrafts is the ability to operate within small spaces such as urban settings. Whereas traditional airplanes have fixed wings that amass a significant amount of space and is a critical design factor for airport infrastructures, VTOLs are similar to helicopters and have rotors that take up minimal room. Currently, there are two types of VTOLs: rotary wing aircraft and powered-lift [30]. Rotary wing vehicles have spinning rotor blades around a mast that supply the aircraft’s lift and thrust. On the other hand, the same source explains that powered-lift vehicles have some form of fixed wing design that is used for direction changes or stable flight [30]. The most advanced VTOLs today are electric and are either electrically charged or powered by batteries. eVTOLs also include both fixed and non-fixed wing aircrafts and have five classifications in itself: vectored thrust, lift and cruise, wingless (multirotor), hover bikes and personal flying devices, and electric helicopters [31].

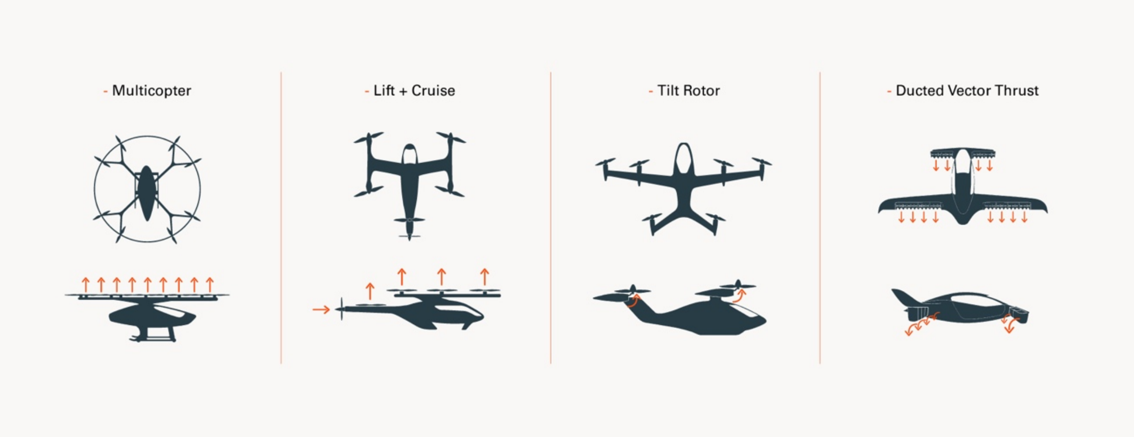

Figure 3: Different types of eVTOL. Source: [4].

2.4.1. Taxiing

With eVTOLs development in view, manufacturers are also looking into different types of taxiing functions for aircraft movement on the helipad. In conventional airplanes, active taxiing uses wheels to steer the aircraft towards or away from the runway using its own power. Requiring approximately 65 gallons of fuel to taxi a single-aisle jet, taxiing is cost-intensive and releases emissions into the environment [32]. Increased aircraft weight due to additional fuel also results in higher fuel consumption during flight. Therefore, the concept of electric taxiing was developed and divided into two categories: external systems and on-board systems. A common example of an external system is the TaxiBot, which is likened to an electric tractor and functions as a tow in all taxiing procedures (pushback, taxi-in, and taxi-out) and is referred to as “passive taxiing” [33]. This semi-autonomous hybrid vehicle is primarily controlled by the pilot, is composed of two diesel engine, and can tow up to 500 kW. TaxiBot is the “only certified and operational taxiing solution in the world” [34]. According to the same source, on-board taxiing systems use electric motor power converter and electric energy to supply power to its wheels. In 2005, WheelTug became the first company to develop this on-board taxiing system, and as of July 2021, began its manufacturing process in the US [35]. Independent of physical tugs or engines, WheelTug endeavors to cut 5 to 20 minutes of vehicle turnaround time on the ground.

2.4.2. Hovering

eVTOLs are equipped with a hovering capability, which uses spinning blades to create vertical thrust [31]. Movement horizontally, forwards, or backwards also uses rotors such as tiltrotors to direct its thrust towards the direction of movement. Nathan et al. classifies eVTOL into four categories: aircrafts with multicopter (multirotor) architecture, lift and cruise architecture, tilt rotor architecture, and ducted fan architecture [36]. Multirotors, which are aircrafts without wings, lack cruise efficiency and thus can only sustain hover for short periods of time, limiting their application to UAM markets only. Winged eVTOL aircrafts has the “lift and cruise” architecture, which leverages both its rotors and wings to achieve robust vertical takeoff and landing and efficient cruise. Thirdly, eVTOLs with tilt rotor architecture are aircrafts with tilting propellers either with or without wings. The tiltrotors enable the vehicle to rotate 90 degrees when transitioning from a horizontal configuration to forward flight. According to Nathan et. al, a critical disadvantage that comes with this model is higher costs associated with the hover requirement, which calls for large propellers with low tip speed and disc loading [36]. The last category is eVTOLs with ducted fans, which excels in reducing noise and is especially important for aircrafts with higher payloads.

2.5. Battery technologies

The energy source that will power future eVTOL vehicles will most likely come from battery electric propulsion systems [37]. Electric propulsion is a popular choice of energy technology because it releases zero emissions into the environment, a huge advantage in cities. While there are huge environmental benefits, batteries also have limited energy densities and greater weight. Nevertheless, battery technology is the primary means to achieve all-electric vehicles apt for travel in space-constrained urban settings.

Since batteries store energy for later use, the development of sound electricity infrastructure system is a critical factor in building urban vertiports. Electric power generation and the connectivity of existing electrical grids will also pose as significant challenges to vertiport operations. Currently, there is a debate between battery swapping and battery recharging as the two primary methods of supplying eVTOLs with energy.

2.5.1. Battery swapping

The main argument for battery swapping over charging is the technical challenges that battery charging can pose. Firstly, the current capacity of electric generation and power distribution at electric grids are not designed to support large numbers of electric vehicles (EVs) [38]. Additionally, Adegbohun says that fast DC charging of EVs could “critically affect the reliability and stability of the power grid” [38]. Load spikes especially during peak-load periods could cripple entire electrical systems. Therefore, Adegbohun concludes that battery charging infrastructure and electric grid integration must evolve rapidly for EVs to be adopted at scale. This induces the need for vertiport infrastructure design to include battery sharing stations (BShS) or battery swapping station (BSS) for battery pack swapping, and potentially a wider battery sharing network (BShN).

Tesla had once designed a BSS system for its cars which includes vehicle lifts, vehicle and electric connection alignment equipment, and battery storage racks [38]. Once an EV arrives, the system is prepared to swap out the battery and replace it with a new one. It was demonstrated by Tesla in 2013 and only shut down due to lack of interest among Tesla owners [39]. However, in China, battery swapping is common among ground vehicles. Nio, a Chinese electric car manufacturer, had launched its second generating battery exchange station in Beijing. It is able to swap 312 batteries per day [40]. Equipped with four collaborative cloud commuting systems and a maximum of 239 sensors, Nio's battery stations is expected to be in operation across its 500 units by the end of 2021. Geely Technology Group is another Chinese company that has already established BSS for automobiles in 39 locations and planning to increase to 200 locations by 2023 [41]. Each BSS will encompass 126 square meters and have the capacity to service over 1,000 vehicles per day. Also according to Geely, the BSS will perform its operation entirely automatically from selecting compatible batteries to handling wireless payments within 90 seconds, paving the way for the development of battery as a service business model for future EVs [41].

Figure 4: Nio's battery swapping station. Source: [5].

2.5.2. Battery charging

Electric vehicle charging has been around since the mid-19th century, yet it was not well developed due to high associated costs. However, investments in space travel in the 1950s propelled interest in battery and electrical charging technologies. In 1997, Toyota made electric charging popular in modern-day society through the release its hybrid EV, the Toyota Prius [42]. Today, EV car charging is very prevalent in China and the United States. China alone utilizes 808,000 EV chargers with its cities taking the lead in EV charging infrastructure, accounting for about 40% of charging posts nationwide [43]. According to the same source, the United States has at least a half million EV chargers, the majority being home chargers, and approximately 5,600 nonresidential EV charging stations hosting over 21,000 charging posts [43]. In Brown et al.'s paper for UAM vehicle design and optimization, battery charging was concluded as one of the main cost drivers in UAM operations [44]. Not only is battery charging expensive, the time it takes to charge may even take as long as the flight mission time. The more powerful a battery charger is, the higher number of flights can be conducted per charge. The author's solution to achieving affordable battery charger is to reduce battery manufacturing cost and increase battery cycle life [44].

2.6. Existing heliport guidelines

The Federal Aviation Administration (FAA) has compiled a concept of operations which include foundational principles, roles and responsibilities, and scenarios and operational threads related to UAM. Its goal is to support "the growth of flight operations in and around urban areas" through envisioning an operational environment [13]. Along with defining critical terms used in UAM operations, FAA ConOps also prescribes the regulatory roles for UAM. The federal authority of aircraft operation in all airspace is the FAA, who is also responsible for maintaining the airspace to be a safe, operating environment. FAA's Air Traffic Control (ATC) monitors airspace communication to prevent collisions between aircrafts in the National Airspace System (NAS) and thus has access to UAM operational data. However, FAA ConOps also defines an "airspace volume defining a three-dimensional route segment" as a "UAM Corridor," in which "tactical ATC separation services" are not provided. Within these corridors, aircrafts must meet performance requirements and operational rules of corresponding UAM airspace environment.

2.6.1. Heliports

The FAA outlined specific design requirements for heliports and drafted an advisory circular to address the standards. Vertiport infrastructure dimensions, such as Touchdown and Liftoff Area (TLOF), Final Approach and Takeoff Area (FATO), safety area, and approach and departure path in the present study are defined based upon the recommendations of FAA's heliport advisory circular. In AC 150/5390-2C, regulations also address heliport operating requirements for commuters and on-demand operations as well as rules governing its passengers. The design standards apply to "general aviation," which are "flights conducted by operators other than Title 14 of the Code of Federal Regulations (CR) Part 121 or Part 135 certificate holder" [45]. General aviation refers to helicopter operations that do not have scheduled passenger service, and its heliports can be either privately or publicly owned.

2.6.2. Existing vertiport concepts

Additionally, the FAA released a vertiport design guide, AC 150/5390-3, in 1991 for the purpose of guiding planners and communities through developing civil vertiports or vertistops [46]. The standards are recommended guidelines and are mandatory in the case of vertiport projects receiving Federal grant-in-aid assistance. Specifically, the minimum requirement for TLOF is one “tip-to-tip span,” which is the “span between the extreme edges of the plane generated by spinning rotors or proprotors” [46].

2.6.3. Air Traffic Organization (ATO)

Furthermore, the FAA developed an Air Traffic Organization (ATO) policy to establish procedures that must be followed by air traffic control service providers [47]. The ATC system outlined in this policy is to ensure safe, orderly traffic flow free from collisions and to provide relevant control services in certain cases. Related to aircraft takeoff and landing in particular, the ATO policy allows simultaneous operations to be conducted if they are separated by at least 200 feet.

2.7. Vertiport state-of-the-art

UAM has been a highly popular subject in the transportation world, yet exploration around vertiport operations is only a recent pursuit. Though its primary application is to serve the urban landscape, UAM is envisioned by some as an “on-demand air transportation within core urban areas and residential suburban destinations outside city centers using new, electric-powered, vertical takeoff and aircraft” [48]. Cities cannot accommodate large airports; therefore, the development of vertiport is critical for UAM realization.

2.7.1. Vertiport infrastructure

There are currently several key players in the eVTOL and even in the flying car industry; however, there hasn’t been the same degree of advancement in the pursuit of eVTOL infrastructure [6]. Heliports, the infrastructure for helicopters, hold the same idea as vertiports but is not designed to serve on-demand, inner-city operations. One recent publication by Vascik and Hansman introduces a topology design of four classes of vertiport layouts that “determine[s] capacity and sensitivity of throughput to topology and situational parameters” [6]. Vascik and Hansman describe their motivation for vertiport infrastructure research as the means to gain a better understanding of the throughput capacity of operating vertiports. Additionally, Daskilewicz et al. uses an integer program to locate the placements of vertiports that would maximize time savings potential within cities [49]. This program uses locations of households and workplaces to model actual commuting trips that would use VTOLs as the primary mode of transport. Hurdles for

UAM to be realized are many, and infrastructure is a key constraint that will remain a prioritized topic in the years to come.

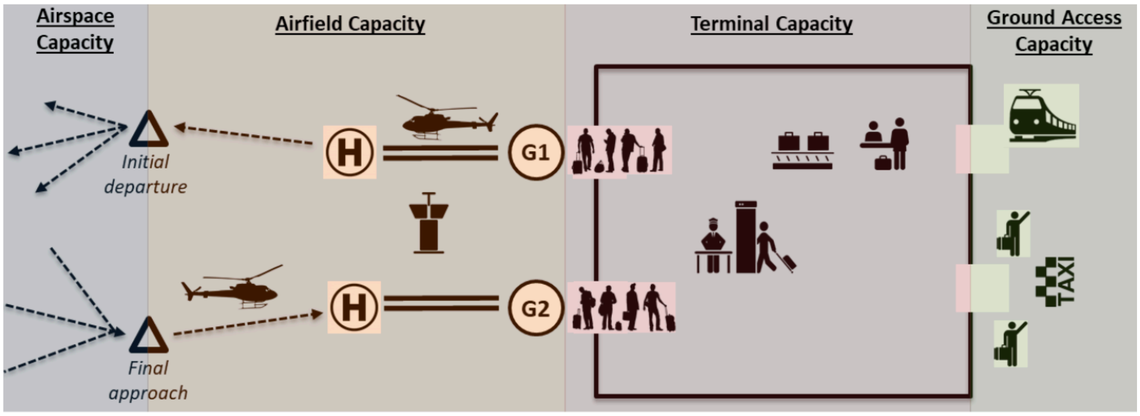

Figure 5: Diagram of a basic vertiport layout with associated operations. Source: [6].

2.7.2. Vertiport operations

While there is increasing attention on infrastructure design, there is still little research conducted around the behavior of vertiport operations itself [15]. Existing heliports serve helicopters and are characterized by similar procedures as future vertiports, yet vertiports differ due to the unique needs of electric vehicles. eVTOLs are fully electric and hence require facilities that can accommodate capabilities such as charging or battery swapping. The progressive next step is to investigate critical design factors and driving processes required to adequately support a fully operational vertiport.

2.7.3. Existing vertiport prototype

There are numerous companies currently developing eVTOL technology and aircrafts, yet there has only been one successfully built working vertiport infrastructure– the VoloPort, the result of a collaboration between German company Volocopter and London-based Skyport. Built in 2019 in Singapore, the prototype achieved real-life testing of entire passenger processes, including pre-flight checks, passenger lounges, and boarding procedures [50]. They also used the Voloport to observe vertiport operations such as battery swapping and charging, maintenance, safety, and security. The Voloport was built primarily for testing purposes and is currently not operational; however, Volocopter and Skyport plan to continue their cooperation to realize commercial air taxi services within two to four years [51]. There are several companies who have plans to develop vertiport infrastructure in the near future, phasing into the next leg of the race for UAM realization. Even locations, namely Miami and Orlando, have been identified as prospective metropolitan areas that could be used to test early UAM flights [52].

Figure 6: The Voloport in Singapore. Source: [7].

2.8. Vertiport model and simulation framework

Currently, there is literature that models the potential demand of UAM using defined networks and vertiport locations [53]. However, not many have conducted studies that account for dynamic effects occurring within vertiport infrastructure. Therefore, this thesis will be based on the most recent and relevant study on vertiport ground operation, a study that introduces an agent-based simulation framework extended from Vascik and Hansman's vertiport concept and co-developed by Preis and Amirzada [8].

The vertiport model in Preis' paper uses Agent-Based Modeling and Simulation (ABMS), a transportation simulation framework. Inputs of the simulation are the vertiport layout, initial positions and states of the agent population, a list of executable plans, and outputs describing vertiport operations over the course of a day including waiting times. It consists of three elements: pad, gate, and stand, with the terminal and airspace acting as the system boundaries of the model (see figure 7). There are two agents, passengers and vehicles, whose locations are updated with every action according to the timestep. Agents contain information on its parameters, position, and destination and moves according to on-demand arrival and request inputs. Each simulation begins with a population of passengers and vehicles, and at any point in time, the simulation can output the location and states of each agent. Consequently, this model can delineate the schedule of vertiport operational processes given its demand, and therefore predict the throughput and operational limits. A parallel study regarding vertiport layouts is also currently underway to serve as an extension to the inputs of this model.

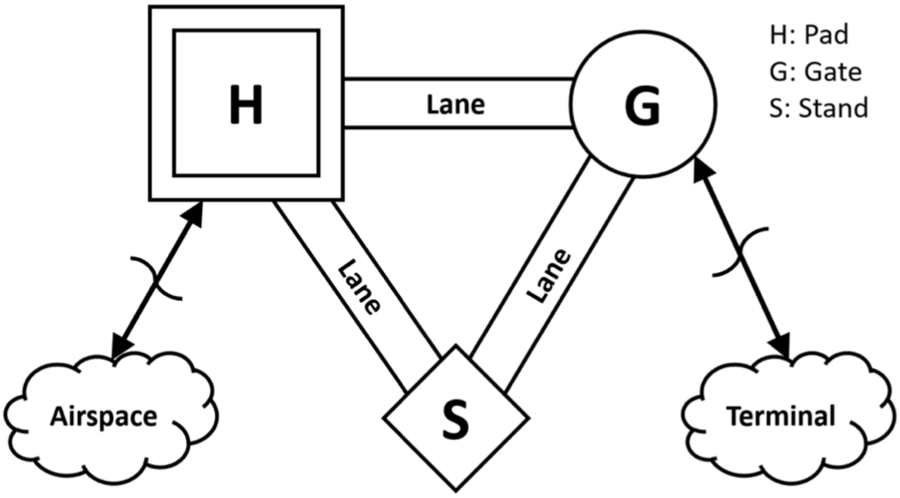

Figure 7: Vertiport model from Preis' vertiport simulation. Source: [8].

2.8.1. Existing vertiport simulation

Two machines define the movement and states of the simulation's agents. The motion machine reads a plan which directs the agents' movements among the elements. The state machine defines the condition of each element at any given time. In the simulation, passengers can be in the states of waiting/occupied and moving, while vehicles have two additional states of being free/available or busy. The simulation elements too have states of being free/available or occupied/moving. Table 1 depicts all the possible combinations of agents' states at any given timestamp.

State	Element	Vehicle	Passenger
Free/Available	x	x	
Busy		x	
Waiting		x	x
Occupied/Moving	x	x	x

Table 1: List of possible states for elements and agents from Preis 2021. Source: [8].

2.8.2. Operational parameters

Movement of agents are solely dependent on the value of their respective parameters. In his paper, Preis lists the basic parameters that characterize each agent as estimated by experts. He focuses on boarding and deboarding procedures, passenger walking time, vehicle takeoff and landing time, and vehicle taxiing speed (see table 2). The value for agent parameters defines the microscopic movements within the simulation and ultimately controls the amount of throughput that can be achieved in any given vertiport.

Parameter	**Value**	**Unit**
vehicle taxi-speed	2.2	m/s
vehicle takeoff time	60	s
vehicle landing time	60	s
passenger boarding time	30	s
passenger deboarding time	25	s
passenger walking from terminal to gate time	20	s

Table 2: List of parameters estimated by experts from Preis' vertiport model. Source: [8].

3. Methods

This study seeks to determine:

- The critical designs and processes that occur on a vertiport
- The parametrization and quantification of these processes
- The effects of calibrated parameters on the vertiport simulation

Whereas Preis' vertiport simulation inputs only included values found in literature review, the following research involves expert estimations of parameters to capture more current, realistic vertiport operational values. Through novel deterministic and stochastic models, these parameters were consequently used as more refined inputs in the vertiport simulation to produce more accurate behavior of vertiport operations.

3.1. Scientific expert interviews (methods)

Expert interviews, commonly used as a method to obtain information in specific subject areas, were held across different aviation-related industries to identify critical vertiport designs and processes as well as values of critical parameters involved in vertiport operation. According to Meuser and Nagel, an expert is a "person who is responsible for the development, implementation or control of solutions/strategies/policies" and a "person who has privileged access to information about groups of persons or decision processes" [54]. Bogner, Littiz, and Menz classified expert interviews into explorative, systematizing, or theory-generating interview, and the author chose to conduct systematizing expert interviews for the purposes of this study. Whereas explorative interviews provide orientation about new fields of research and theory-generating aims to challenge social constructs, systematizing interviews perform systematic retrieval of information [55]. Furthermore, they focus on the exclusivity of expert knowledge, are used for information not widely accessible, and emphasize on comparison and aggregation [56]. Through systematizing interviews, the author obtained estimated parameter values from various experts and created a model to aggregate their responses for every parameter of interest.

There were 17 experts who participated in the interview series from three nationalities (German, US, Great Britain) and multiple backgrounds: research, aviation industry, aircraft operation, and architecture. This group of experts have an average of 10.8 years of experience and a median of 6 years. All interview durations were 30-45 minutes and conducted virtually, predominantly in a face-to-face format using internet video conference tools. Information discussed remain strictly confidential and only data was extracted from each interview with experts.

Expert interviews were held in two rounds. The first round included the initially determined parameters and the second round had more targeted, critical parameters that were identified through an iterative process between the first and second rounds (to be described more in section *Parameter determination*).

Expert determination

Experts were located primarily through previously established contacts in the aviation industry. However, to reach a larger audience and industry background, experts were also found through an online professional networking site, LinkedIn. These interviews were conducted throughout a six-month interval; all the contacted experts who replied or showed interest to the study during this time window were given the opportunity to have their parameter estimations included in our research.

Pre-interview procedures

Prior to interviewing the experts, critical parameters had to be preliminarily identified without the aid of expert inputs. Although an iterative process of parameter determination was ongoing throughout the interview series, the set of parameters presented to the first round of experts were critical parameters identified in literature. These parameters were presented to the experts as a Microsoft Word document that contained empty blanks to be filled in with estimated values by the experts. For this purpose, there was a preliminary, small-scaled literature review of research regarding vertiport infrastructure, operations, passenger processing, and battery technology.

The first contact with the experts is an initial email introducing the interviewer, research subject, and purpose of interview. The subject is invited to participate in the interview and an interview guide is sent to the expert. As a gesture of gratitude, the expert is then offered a “sneak peek” of the final data obtained from all the experts at the conclusion of the series upon agreement to be interviewed. If the expert responds to the initial email with an affirmative, available dates and times is then offered to him or her along with a data consent form for the interview to be recorded for data processing purposes. The experts who do not agree to have his or her interview recorded do not have to sign the data consent form and will just proceed to be interviewed without recording. After the expert responds a second time, a conference link is then sent out to him or her.

Interview structure: first round

Previous work included 10 interviews already conducted within the first round. Each interview consisted of the following four sections: *General Information, General discussion of Urban Air Mobility, Discussion of Vertiport model, and Vertiport simulation parameter estimation*. Depending on the expert, interviews were conducted in English or German. Then in the first section, *General information,* the interviewer confirms with the expert that he or she had consented to being recorded and had returned the data consent form signed and dated. Afterwards, the interviewer writes down the name of the interviewed person, the affiliation with his or her institute, background and field of work, years of experience, and reason for participation. Next, in section two, *General discussion of Urban Air Mobility,* the interviewer asks a series of questions and provides some input regarding the definition of UAM, potentials, and challenges of UAM.

Section three consists of a discussion of the vertiport model, wherein the interviewer gives an explanation of the model through previously prepared Microsoft Powerpoint slides, which serves as the context of the present research. Questions regarding the expert's evaluation regarding the critical design driver or missing elements in the model is discussed here. Also, the initial parameters of interest were grouped and experts were asked about the suitability of each grouping. In section four, all experts were introduced to the same list of parameters and requested to fill out a parameter form with his or her predicted values for each parameter and email the response back. Specifically, experts are asked to estimate a mean value, minimum value, and maximum value with respective units. Next, they are asked to rate the confidence of their responses on a scale of one to three, 1 being "very sure," 2 being "sure enough," and 3 being "educated guess." Lastly, final questions include asking the expert to identify the most important parameters on the parameter list, parameters not on the list yet are also critical, and additional input that is essential to the topics discussed in the whole interview. The interview ends with the interviewer thanking the expert for his or her time and reminding them to be on the lookout for a summary of anonymized results from all the interviews in the near future.

Interview structure: second round

The main difference between the interview structure of the first and second rounds is the set of questions in the interview guide. The second round of interviews were conducted by the author and consists of seven experts. The interview guide has the following four sections: *General Information, General discussion of Advanced Air Mobility (AAM), Vertiport model and parameter discussion, and Parameter estimation* (see appendix 1). In part two, the general discussion changed from UAM to AAM because the latter encompasses a broader mobility application than just cities. Part three eliminated discussion purely around the vertiport model to focus on parameter discussion, using the developed vertiport model as the context. Here, the experts were presented Powerpoint slides of groups of parameters related to vertiport operations (see appendix 2). They were then asked to identify the parameter from the group that is most influential from an operational perspective and other parameters that were found worthy of consideration. This leads to the next part, *Parameter estimation*, which asked for similar estimations of parameter values as interviews in the first round. The only difference is that in the second round, experts were only asked about values that were directly relevant to his or her research. Thus, part three introduced only the parameters and parameter groups that will be asked of the experts in part four.

Post-interview analysis

The research data gathered in each interview can be broken down into three main parts: UAM/AAM insight, vertiport model and parameter discussion, and parameter estimation. The first section, UAM/AAM insight, were primarily used to understand the perspective of the expert's industry or background experience. The second section was for obtaining expert feedback regarding the vertiport model and to provide a framework for experts to understand the parameter values needed in the vertiport simulation. Thirdly, in the section for expert parameter estimation, the data obtained was used as the primary input for the stochastic model developed in this thesis. In the methods section "Stochastic modeling," a detailed description of how this data was used to establish the model will be provided.

Interviews that were recorded were transcribed post-interview for further data analysis. The UAM/AAM responses were recorded in an Excel sheet with four tabs: "Definition of UAM," "Realization of UAM," "UAM Potentials," and "UAM Hurdles." For "Realization of UAM," responses were categorized by expert name, a yes or no answer to whether or not UAM will be realized, the year it could be realized, and remarks related to the expert's prediction. For UAM definition, realization, and hurdles, expert responses were categorized by common field-related keywords related to each of the three concepts. If the expert's response included a keyword, then that field was marked and consequently totaled to reveal experts' aggregated response. Keywords used per respective section are shown in table 3. The aggregation of these expert responses were summarized into a "sneak-peak" presentation and sent to all the participating experts as a gesture of gratitude.

The second part, vertiport model and parameter discussion, included an evaluation for both the vertiport model and associated parameters. Responses to the questions regarding present and missing critical design factors in the vertiport model were recorded. Specifically, expert responses for the following items were documented: design driver and critical path, model sufficiency, safety threats, and other remarks. Furthermore, experts' inputs on the critical and missing parameters and their additional inputs contributed to the formation of parameter groups.

Lastly, a sneak peek of aggregated expert responses concerning UAM, AAM, vertiport model, and parameter groupings was sent out to the participating experts as a thank you (see appendix 3 for selected slides from sneak peek). It was compiled in a Powerpoint presentation, in which the data sources remained anonymous and confidential. Further analysis regarding UAM/AAM potentials and hurdles were depicted in bar graphs, and the most common responses for critical factors or parameters for vertiport infrastructure and vertiport operations were presented.

Definition of UAM	UAM Potentials	UAM Hurdles
noise/quiet	congestion	battery capacity
one leg in city	enrich transportation system	flight authorization for vehicles
VTOL	remote areas	safety
inner-city	urban transport	noise
air taxi services	fast travel	space in cities
ODM	cargo	community acceptance
electric/hybrid	autonomy	electric/hybrid
range	link suburban cities	range
autonomous	energy efficiency	autonomous
affordable for public	emergency transport	affordable for public
thin haul	city center to airport	competition with conventional modes
metropolitan	business/fast travel	privacy
reduce pollution	technological advancement	ATC
on-demand	relaxes urbanization	infrastructure/integration
urban	new market	regulation/policy
sub-urban	urban planning	business model
UAVs	democratization of airspace	system dynamic
cargo	airport connection	airspace structure & ATC
multimodal	cargo luxury goods	vertiport
safety	time savings	visual pollution
complex (airspace)	experience	user acceptance
3D mobility	maintenance business	access & egress
regional	goods transportation	vehicle technology
shared	remotely controlled air transport	-
AAM	regional air mobility	-
-	help developing countries	-

Table 3: Keyword responses regarding UAM definition, potentials, and hurdles.

3.2. Parameter determination (methods)

This section, *Parameter determination,* describes actions that were performed from before the initiation of expert interviews up until, and including, post-interview analysis. As mentioned previously, parameter values that were presented to the experts for estimation were determined preliminarily through an initial round of literature review in prior work. The first draft parameters list, compiled in previous work, included 82 parameters sectioned into 10 “top layer” processes: vertiport elements, passenger processing, passenger boarding, vehicle taxiing, takeoff and landing, approach/departure flight, battery charging, battery swapping, vehicle maintenance, and general vertiport operation. Among the 82 parameter, 18 parameters were initially selected as the driving parameters for the baseline vertiport simulation model. However, a combination of the 82 parameters were introduced to the first round of expert interviews in the questions involving the vertiport model, vertiport operations, and parameter estimation.

After the first round of interviews, previous work discovered that some of the parameters presented to the experts were either sufficiently answered by literature, irrelevant to the model, or too general. Sufficiency of number of answers was assessed through analysis of the number of responses and the average of the confidences of expert responses. To identify irrelevant or over-generalized answers, as described previously in *Interview structure: first round,* experts were asked to point out the parameters that were most critical or missing. Thus, through deletion and combination of certain parameters, the list of 82 parameters was narrowed down to 55 parameters of interest, in which 25 parameters will be essential to the model (see appendix 4 for example of elimination process*)*. Of the 25 parameters, 4 are related to the creation of the vertiport mode elements and 21 are related to guiding operations.

Before the start of the second round of interviews, a Microsoft Excel sheet was created to organize all the expert responses thus far according to standardized units and parameter IDs. In the process, the number of responses for each parameter was summed up. The totals produced from that assessment revealed the parameters that were adequately answered and those that were lacking in responses. Thus, the second round of interviews included only the 25 essential parameters derived after the first round of interviews with emphasis on the 9 parameters that were found to have 1 or less responses. 4 of these 9 parameters are related to vertiport layout elements, which could be sufficiently answered with further literature review. The remaining 5 parameters that were lacking in responses were specifically taken into account during the search of experts from appropriate disciplines for the second-round interviews.

After collecting responses during the second round, total expert responses from the first and second rounds were summed and final parameters were determined. Two steps were taken here: firstly, an evaluation of the accuracy of expert responses to parameters was conducted to ensure quality of data. Secondly, parameters with 5 or more responses had its minimum and maximum values eliminated to rid outliers and to achieve closer-to-average and median distributions. In the first step, excluded responses were either irrelevant or inadequately answered by the experts. The following points are examples that illustrate the determination process for selected parameters:

- Passenger board helicopter: Expert A defined distinct values for passenger stepping into helicopter, storing luggage, and sitting down and buckling the seatbelt. Therefore, these values are aggregated to define the parameter *passenger board helicopter.* The confidence value is determined by the majority response. Expert B provided values of passenger stepping into helicopter and sitting down and buckling the seatbelt, which were similarly aggregated to maintain consistency as best as possible. Expert C is also excluded because the expert defined values for passenger boarding of an airplane rather than a helicopter.

- Starting Rotors: The vertiport simulation is modeled for electric helicopters. Since Expert D and Expert E defined values for starting rotors of conventional helicopters, their responses are not included in the stochastic model. Expert F and Expert G's values are for electric helicopters and are included in the model.

- Initial hover: The response for Expert H is excluded from the stochastic model because the value represents the time it takes for the airspace around the pad to be cleared for the next vehicle to land or takeoff rather than just the initial hovering time required before takeoff.

- A/C Separation: Expert J defined values for wake vortices, which is not interesting for this study and therefore excluded. Rather, A/C Separation parameter refers to the separation minima (time) between aircraft activities on the airfield.

There was 1 parameter value, battery swapping time, of the 25 that remained unable to be estimated by any of the experts. So that parameter was ultimately excluded from the final parameter list of 24, which were the inputs for the stochastic model.

3.3. Deterministic modeling (methods)

As introduced before, there will be 5 vertiport simulations conducted using Preis' vertiport simulation model, 2 of which using deterministic inputs. These inputs include both expert estimations and literature findings of parameters. Previous work established initial input parameters for the model through a preliminary round of literature review. Now, for producing a more refined list of parameter input for the deterministic model, a second round of literature review was conducted and averaged with the newly-obtained expert estimation values.

A more extensive search for related parameter values in literature was performed and results were recorded in an Excel spreadsheet. To ensure quality of data and accuracy of responses, each value was kept only if it exactly fit each of the final 24 parameters. Next, obvious outliers were eliminated. After obtaining the list of literature parameters, the values were ready to be combined with the list of 24 expert responses. This process uses the method of weighted averaging for each parameter, which sums the multiplication of the number of expert and literature entries with respective averages divided by the total number of entries (equation (1)). The final, averaged list can be found in table 7. The resulting list of 24 parameters is used as input parameter values for the deterministic model in the vertiport simulation.

$$\Sigma(no.entries * average)/(total\ no.entries) \tag{1}$$

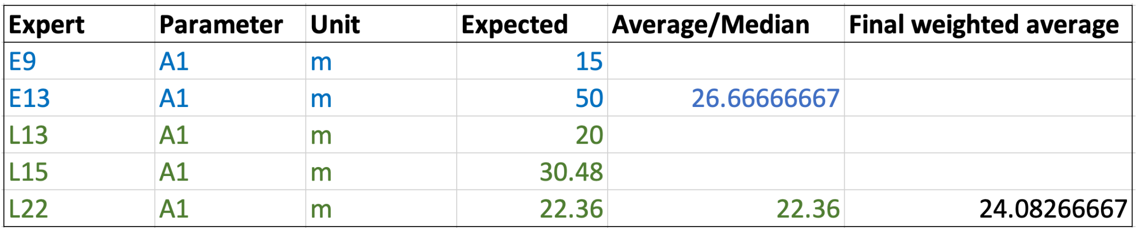

Expert	Parameter	Unit	Expected	Average/Median	Final weighted average
E9	A1	m	15		
E13	A1	m	50	26.66666667	
L13	A1	m	20		
L15	A1	m	30.48		
L22	A1	m	22.36	22.36	24.08266667

Table 4: Example of weighting between literature and expert values.

3.4. Stochastic modeling (methods)

The second vertiport simulation uses inputs that are determined stochastically. Expert estimations for parameters were gathered through expert interviews, and these responses were processed through normal distribution and skew normal distribution models to be prepared as inputs for the vertiport simulation. This section will describe the background mathematical basis for the methods employed to stochastically model the expert responses, the methods themselves, and the preparation of data as inputs into the vertiport simulation.

3.4.1. Mathematical basis

A normal distribution, or a probability density function (PDF), is a symmetrical, continuous parabolic function that is widely used to represent probability distributions (see figure 8 and equation (2)). Otherwise known as a Gaussian distribution, it holds the shape of a bell curve symmetric about the mean and has an area under the curve of 1. Its function, as shown below, is characterized by a standard deviation and mean of real-value random variables. The x-value of the curve has a y-value probability of occurring. A standard normal distribution is a normal distribution which has a mean of 0 and standard deviation of 1 and is therefore symmetric about the 0. Furthermore, the integral of a normal distribution is a cumulative distribution function (CDF), where each y-value represents the probability for the occurrence of a value equal or less than its corresponding x-value (see figure 9).

In a normal distribution, the values one standard deviation away from the mean represents 68.27% of the distribution, values two standard deviations away represent 95.45% of the distribution, and values three standard distributions away represent 99.73% of the distribution (see figure 10). This function is widely used as it often describes natural phenomena and can be easily interpreted using standard deviation and mean.

$$\phi(x) = \frac{1}{\sigma\sqrt{2\pi}} e^{-\frac{1}{2}(\frac{x-\mu}{\sigma})^2} \tag{2}$$

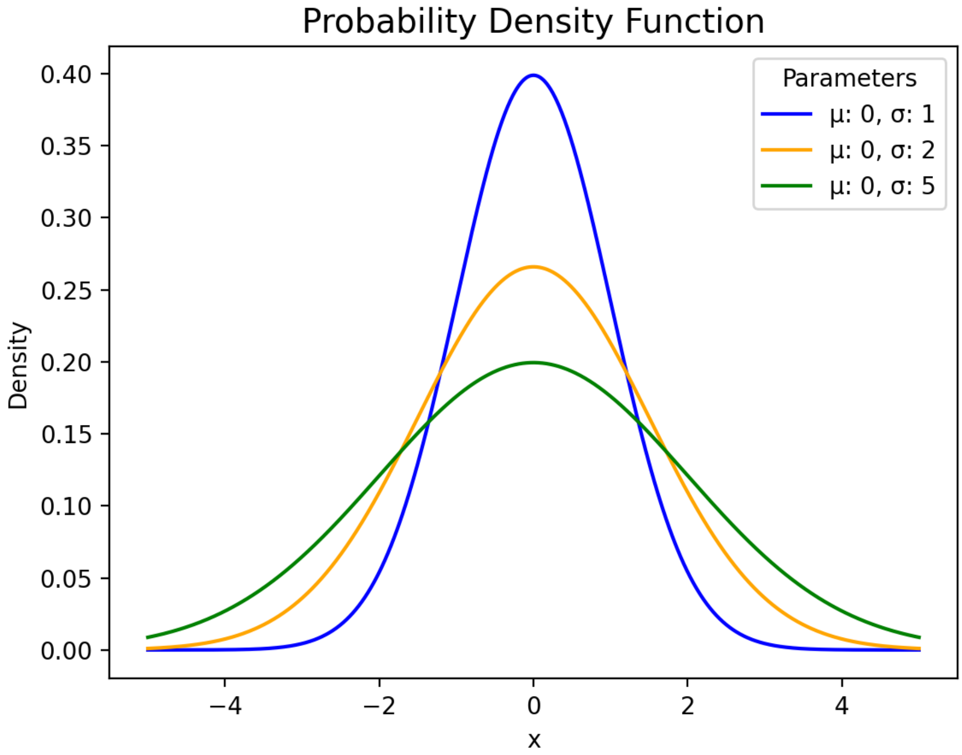

Figure 8: Probability Density Function (PDF) for the normal distribution.

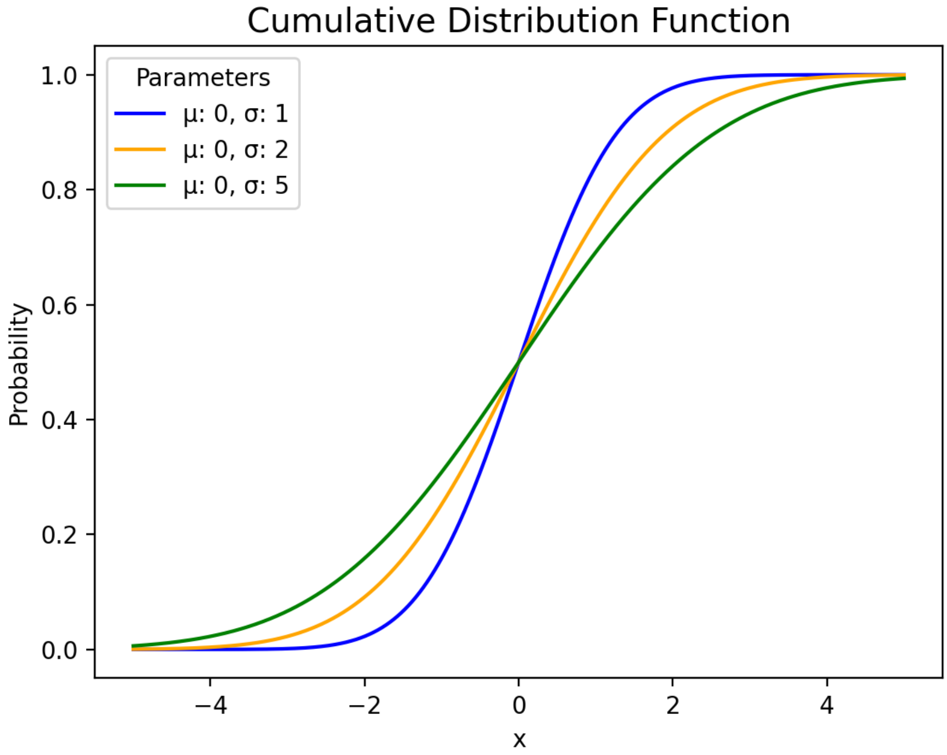

Figure 9: Cumulative Distribution Function (CDF).

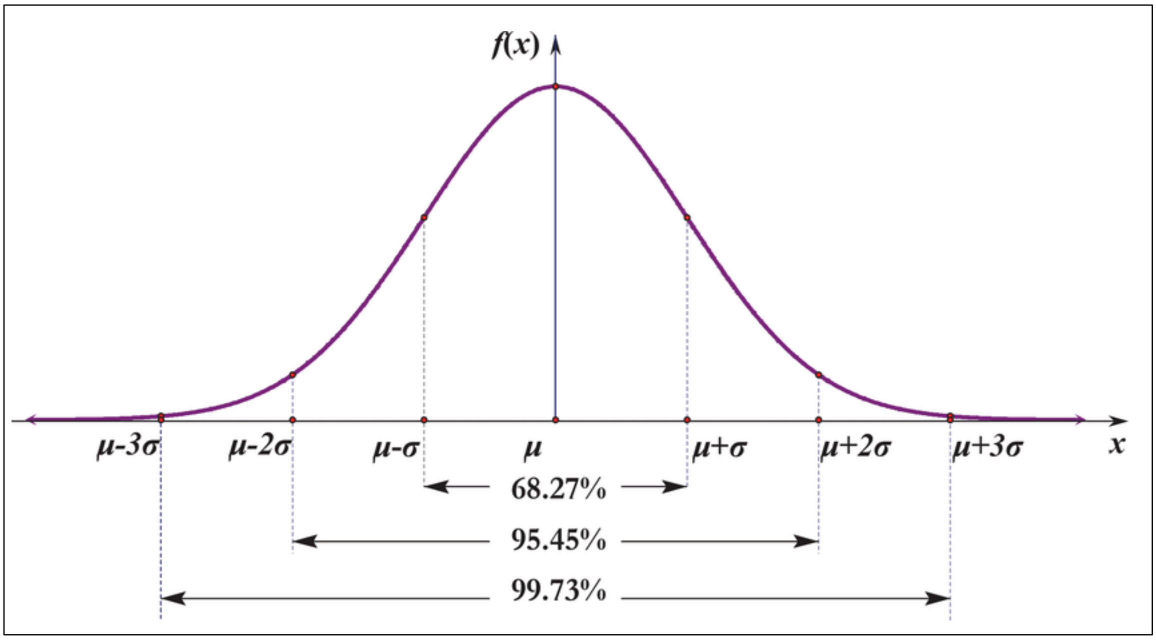

Figure 10: Normal distribution with standard deviations depicted. Source: [9].

A skew normal distribution, on the other hand, is a distribution that is asymmetric about the mean and is skewed left or right. Azzalini defines a skew normal distribution by equation (3), which is two times the PDF multiplied by the CDF [57]:

$$f(x) = 2\phi(x)\Phi(x) \tag{3}$$

Another form of estimation is to reparametrize the density function by a skewness parameter of epsilon ε, referred to as the epsilon-skew normal (ESN) family [58]. Developed by Mudholkar et al., it is denoted as $ESN(\theta, \sigma, \varepsilon)$ and exhibits a unimodal distribution with mode at θ and probability mass $(1+\varepsilon)/2$ below the mode [58]. Each variable represents location (mu), scale (sigma), and skewness respectively, and the distribution reduces to a normal distribution at $\varepsilon = 0$. Equation (4) is the resulting probability density function from Mudholkar et al.'s derivations in its canonical form $ESN(0,1,\varepsilon)$, and equation (5) displays its general form of $ESN(\theta, \sigma, \varepsilon)$.

$$f_0(x) = \frac{1}{\sqrt{2\pi}} \exp\left(-\frac{x^2}{2(1+\varepsilon)^2}\right) \text{ if } x < 0$$

$$f_0(x) = \frac{1}{\sqrt{2\pi}} \exp\left(-\frac{x^2}{2(1-\varepsilon)^2}\right) \text{ if } x \geq 0 \tag{4}$$

$$f_0(x) = \frac{1}{\sigma\sqrt{2\pi}} \exp\left(-\frac{(x-\mu)^2}{2\sigma^2(1+\varepsilon)^2}\right) \text{ if } x < 0$$

$$f_0(x) = \frac{1}{\sigma\sqrt{2\pi}} \exp\left(-\frac{(x-\mu)^2}{2\sigma^2(1-\varepsilon)^2}\right) \text{ if } x \geq 0 \tag{5}$$

3.4.2. Stochastic modeling in Python

The stochastic modeling process in the open-source programming language Python is comprised of three segments: 1) modeling interview responses into skew normal distributions, 2) aggregating skew normal distributions into normal distributions per parameter, and 3) using the previous models to prepare inputs for the vertiport simulation. Lastly, these inputs were implemented into the simulation to produce new observations of vertiport operations.

Modeling interview responses into skew normal distributions

Once the expert responses were obtained with estimated parameter values, minimum values, maximum values, and confidence of answer, a model was built using Python to fit the data into skew normal distributions. The inputs and outputs of this model are as shown in figure 11.

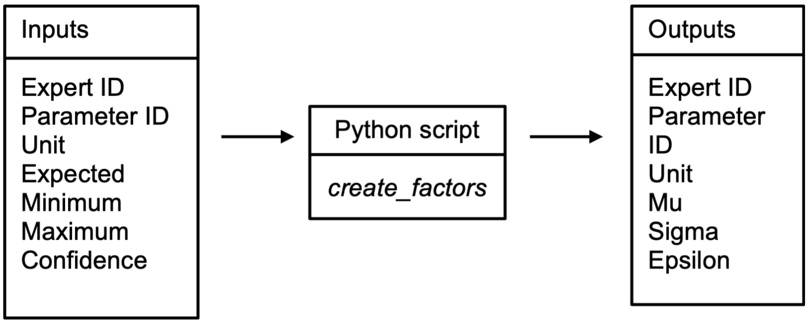

Figure 11: Inputs and outputs of *create_factors*.

The first step of *create_factors* Python script is to read in a comma-separated values (CSV) file of the inputs. Mu (μ), is automatically set to be the expected value, and sigma (σ)is calculated as follows:

$$\sigma = \frac{maximum-minimum}{2(4-confidence)} \tag{6}$$

This was derived from the normal distribution curves (refer to figure 8), where, depending on the confidence, minimum and maximum values were defined to be at a distance of 1, 2, or 3 sigmas away from the mean on the x-axis. For example, if the confidence of an expert response was 1 (most confident), then that expert's estimation for minimum and maximum values would lie on the point 3 sigmas away from the mean in either direction on the x-axis. If the confidence was 3 (least confident), then the expert's estimation for minimum and maximum values would lie on the point 1 sigma away from the mean in either direction. With greater confidence, a greater distribution and probability for the range of estimation was assigned.

For the expert response of each parameter, a skew normal distribution was plotted and the epsilon determined. To find the epsilon, the Mudholkar et al.'s skew normal approximation (equation 5) was defined as a function in the script. The mathematical concept behind arriving at the epsilon is simple. According to a normal distribution function, the x-values of -3 sigmas and +3 sigmas hold the same y-value. It is also observed that the value of epsilon in equation 4 was observed to be greater when $f(maximum)$ is larger than $f(minimum)$ than when $f(maximum)$ is less than $f(minimum)$. Therefore, by initializing epsilon as an arbitrary value of 0.1, a loop is developed for epsilon to:

- Decrease per step when $f(maximum) > f(minimum)$
- Increase per step when $f(maximum) < f(minimum)$
- Continue the iterations until the constraint of $f(minimum) = f(maximum)$ is met (with maximum error at 10^{-4} degree).

The resulting epsilon value is the epsilon associated with each specific set of expert inputs of mean, minimum, maximum, and confidence. This epsilon value is outputted in a CSV file with the respective mu, sigma, and other input parameters.

Modeling each parameter into a normal distribution through aggregation

Having already determined the mu, sigma, and epsilon of experts' estimations for each parameter, the next step was to aggregate all the expert responses and model each parameter into a single normal distribution curve. The inputs of the second Python script, *aggregated_factors,* use the outputs of *create_factors* to produce aggregated skew curves into normal distribution curves per parameter. Using Python's curve fit package "scipy.optimize.curve_fit," this script best fits all the skew normal curves associated with each parameter into one single normal distribution. *aggregated_factors* also outputs the mu and sigma values of the normal distribution curves for each parameter (figure 12).

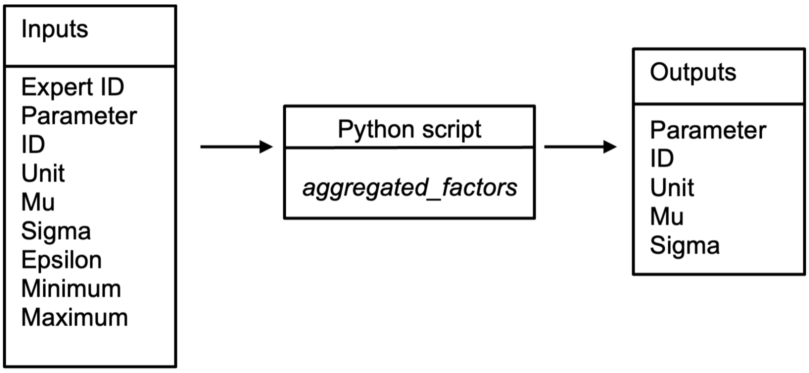

Figure 12: Inputs and outputs of *aggregated_factors*.

The minimum, maximum, and confidence values were added to the inputs to establish the x-limits, or the boundaries of the x-axis, in the plots. These normal distribution curves are the parameter models that will be used to determine the vertiport simulation inputs.

3.4.3. Implementation of model outputs into simulation

Because the vertiport simulation only takes specific inputs, the outputs of *aggregated_factors* must be carefully processed. The current stage of the simulation accepts two input files: arrivals and requests and three output files: arrivals, requests, and starting populations (figure 13). Using the Monte Carlo method of random sampling from each parameter's aggregated, normal distribution, the script *population_generator* begins with 500 vehicles and 1000 passengers as the starting population.

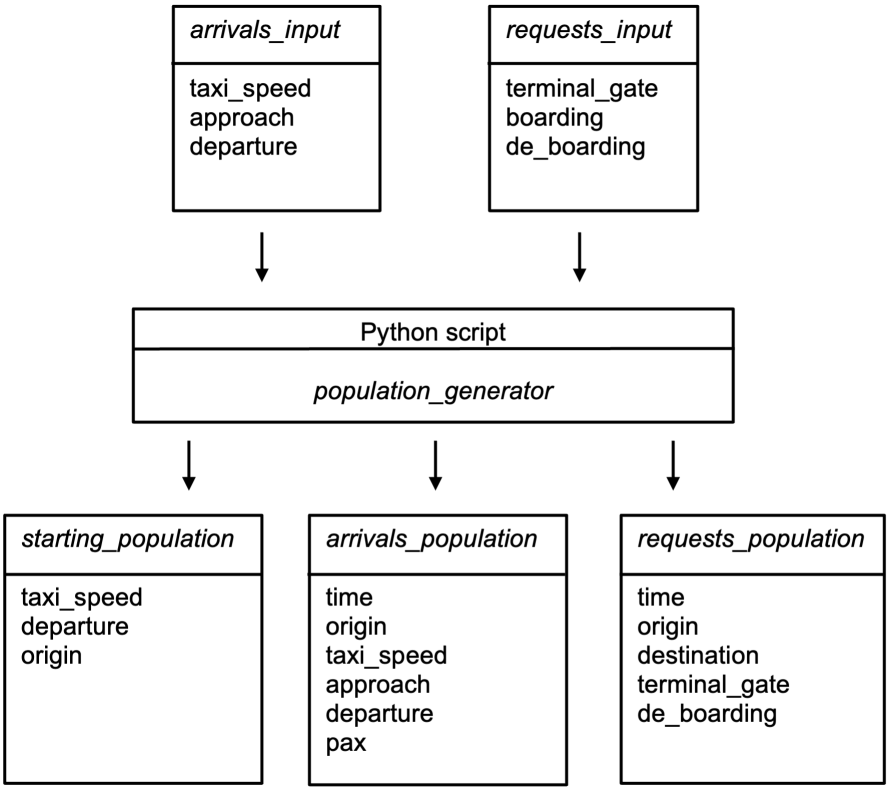

Figure 13: Inputs and outputs of *population_generator.*

In the *arrivals_inputs* file, *taxi_speed* refers to the speed of hover taxiing on the taxiway, *approach* refers to time of stopping rotors, final hover, entering pad airspace, and cooldown, and *departure* consists of time of starting rotors, initial hover, leaving pad airspace, and cooldown. The *requests_input* file involve the *terminal_gate* factor, which is the time it takes for passenger walking from holding place in terminal to the gate. *Boarding* is the time it takes for the passenger to leave the gate and board the helicopter, and *de_boarding* is the time it takes for the passenger to deboard the helicopter and enter the gate. For the parameters that are an aggregation of the original parameters (i.e.

approach, departure, boarding, and de_boarding), the mu and sigma values of respective parameters are summed up to determine the aggregated values.

The output file, *starting_population,* prints the *origin* locations of each vehicle with respective *taxi_speed* and *departure* times. *arrivals_population* and *requests_population* prints the *time* (in seconds), *origin*, and relevant factors that are values of interest in determining the behavior of the agents—vehicles and passengers—at any time during vertiport operations. The times are printed in chronological order, and half the request times are identical to arrival times as these two times overlap when passengers move from pad to terminal upon arrival. One of the output parameters, *de_boarding*, refer to both deboarding and boarding times based upon the direction of passenger travel: from *origin* of airspace to *destination* of terminal or *origin* of terminal to *destination* of airspace, respectively.

3.4.4. Walk-through of stochastic modeling methods

This section will trace through the stochastic modeling process depicted in the methods using an exemplary parameter: C4, passenger deboarding time.

create_factors

After obtaining and processing expert interview data, the expected value (mu), minimum, maximum, and confidence of responses are inputted into the *create_factors* Python script in a CSV file format.

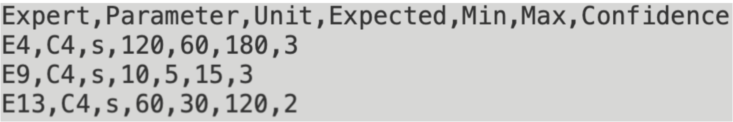

```
Expert,Parameter,Unit,Expected,Min,Max,Confidence
E4,C4,s,120,60,180,3
E9,C4,s,10,5,15,3
E13,C4,s,60,30,120,2
```

Figure 14: Input CSV file of *create_factors.*

create_factors then outputs a CSV file that includes the sigma and epsilon values associated with each expert entry along with some identification information contained in the input files. In addition, skew normal distribution curves were created for each entry. Since there were 3 expert responses for parameter C4, 3 skew normal distribution curves were created based on each expert estimation (see figure 16).

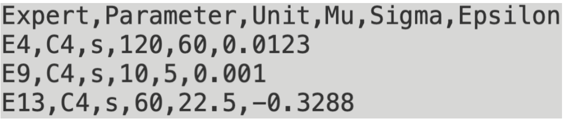

```
Expert,Parameter,Unit,Mu,Sigma,Epsilon
E4,C4,s,120,60,0.0123
E9,C4,s,10,5,0.001
E13,C4,s,60,22.5,-0.3288
```

Figure 15: Output CSV file of *create_factors.*

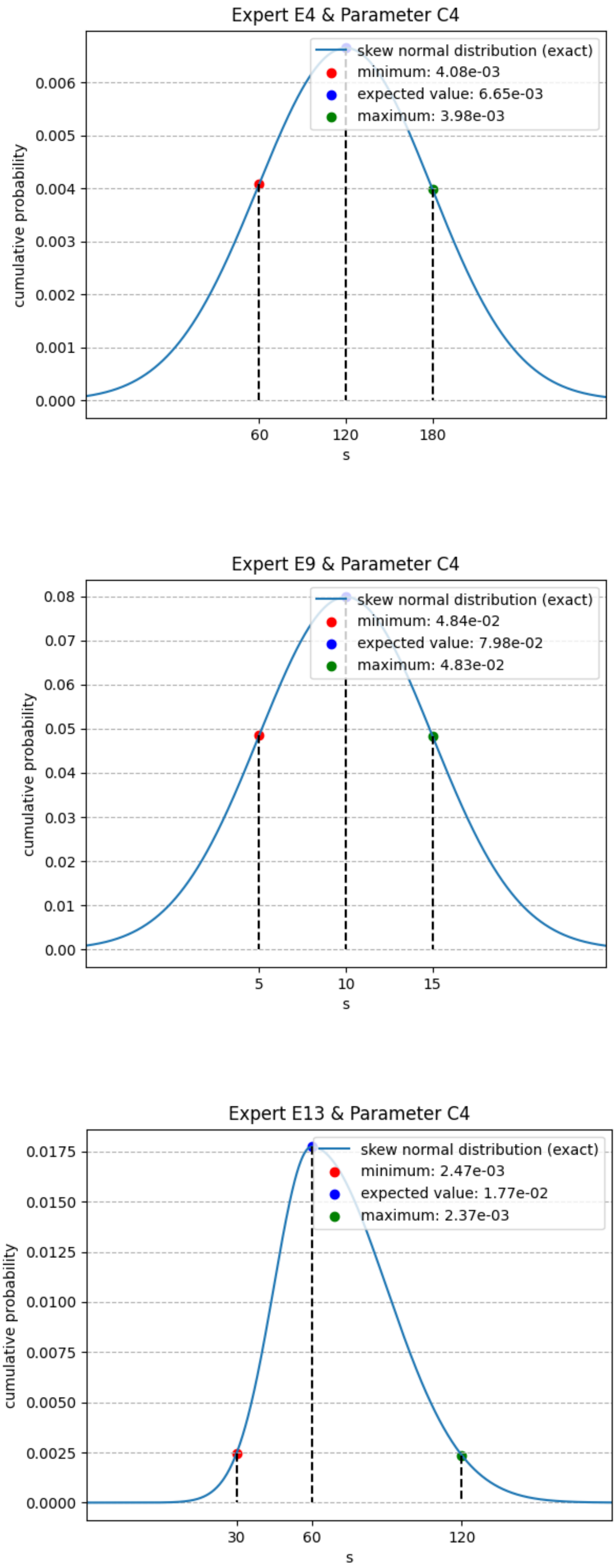

Figure 16: Skew normal distribution curves modeling expert response for parameter C4.

aggregated_factors

Next, the values of mu, sigma, and epsilon were appended with the minimum, maximum, and confidence values respectively to be used as inputs into the *aggregated_factors* Python script. For each parameter, this step generates a normal distribution curve and aggregated values of mu and sigma (see figure 17)**.**

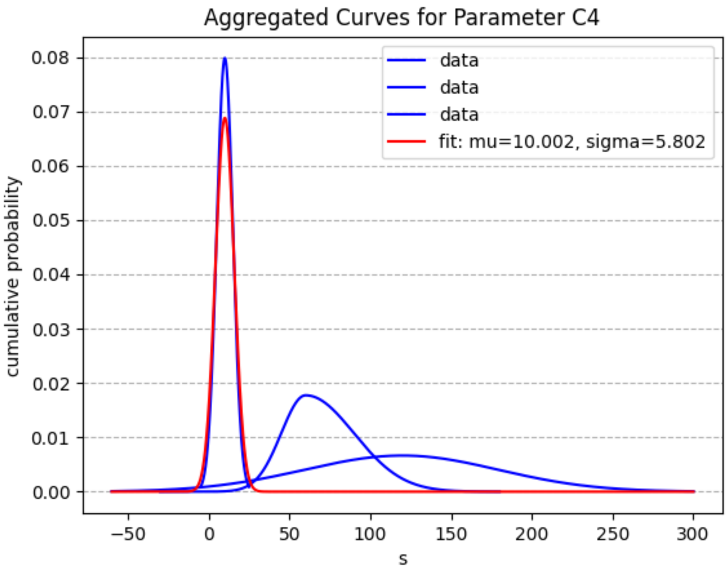

Figure 17: The normal distribution curve modeling all expert responses for parameter C4.

population_generator

With mu and sigma reflecting the normal distribution for each parameter, these values are fed into the *population_generator* script as the “boarding” parameter in one of the input files (the request inputs file ‘*requests_inputs’* in this case). Other parameters, as previously mentioned, are formed by an aggregation of several unique parameters. Outputs of the *population_generator* include a starting population, arrival population, and request population (see figure 18).

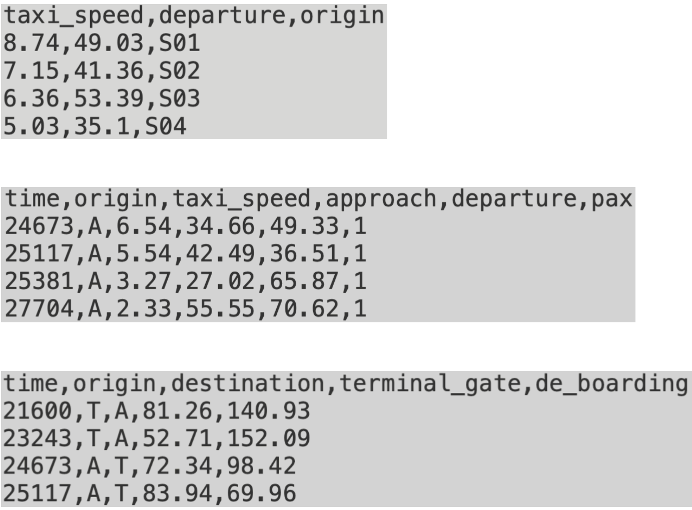

```
taxi_speed,departure,origin
8.74,49.03,S01
7.15,41.36,S02
6.36,53.39,S03
5.03,35.1,S04
```

```
time,origin,taxi_speed,approach,departure,pax
24673,A,6.54,34.66,49.33,1
25117,A,5.54,42.49,36.51,1
25381,A,3.27,27.02,65.87,1
27704,A,2.33,55.55,70.62,1
```

```
time,origin,destination,terminal_gate,de_boarding
21600,T,A,81.26,140.93
23243,T,A,52.71,152.09
24673,A,T,72.34,98.42
25117,A,T,83.94,69.96
```

Figure 18: Top to bottom: starting population, arrival population, and request population as generated by *population_generator.*

Vertiport simulation

These 3 input files, *starting_population, arrival_population,* and *request_population* are the input files used in the vertiport simulation to determine occupancy, agent availability, and variables related to vertiport demand. These topics will be further discussed in Results and Discussion sections.

4. Results

4.1. Scientific expert interviews (results)

The responses of the experts for the qualitative questions regarding UAM and vertiport is displayed in figure 19. More results can be found in appendix 3.

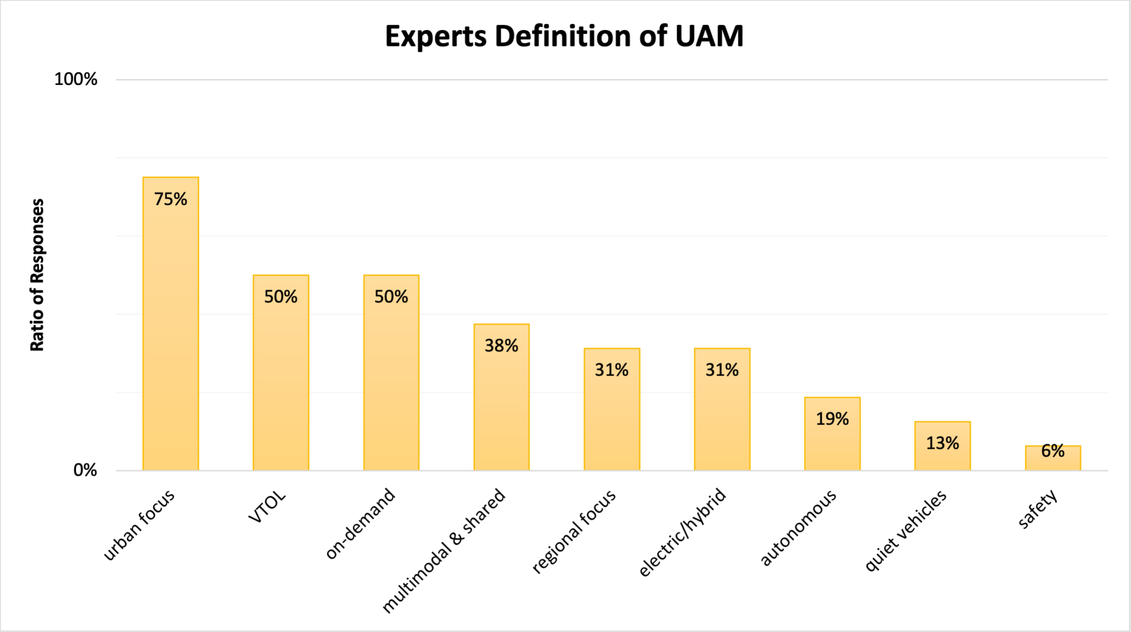

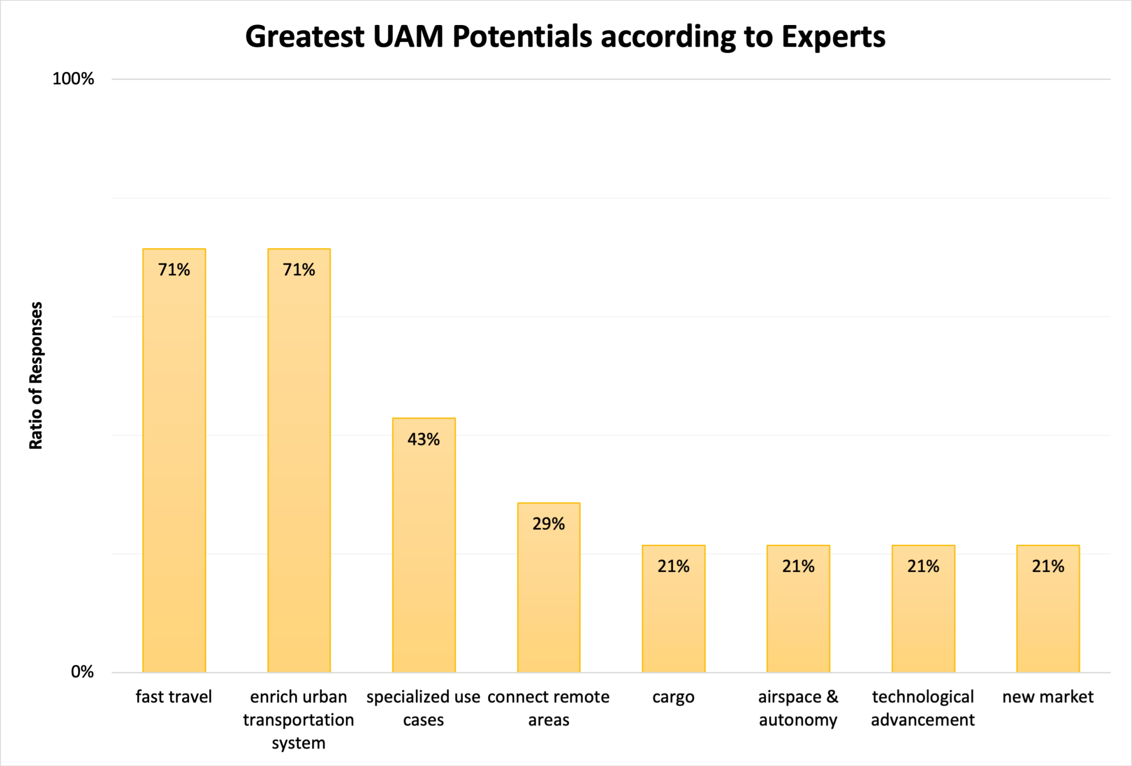

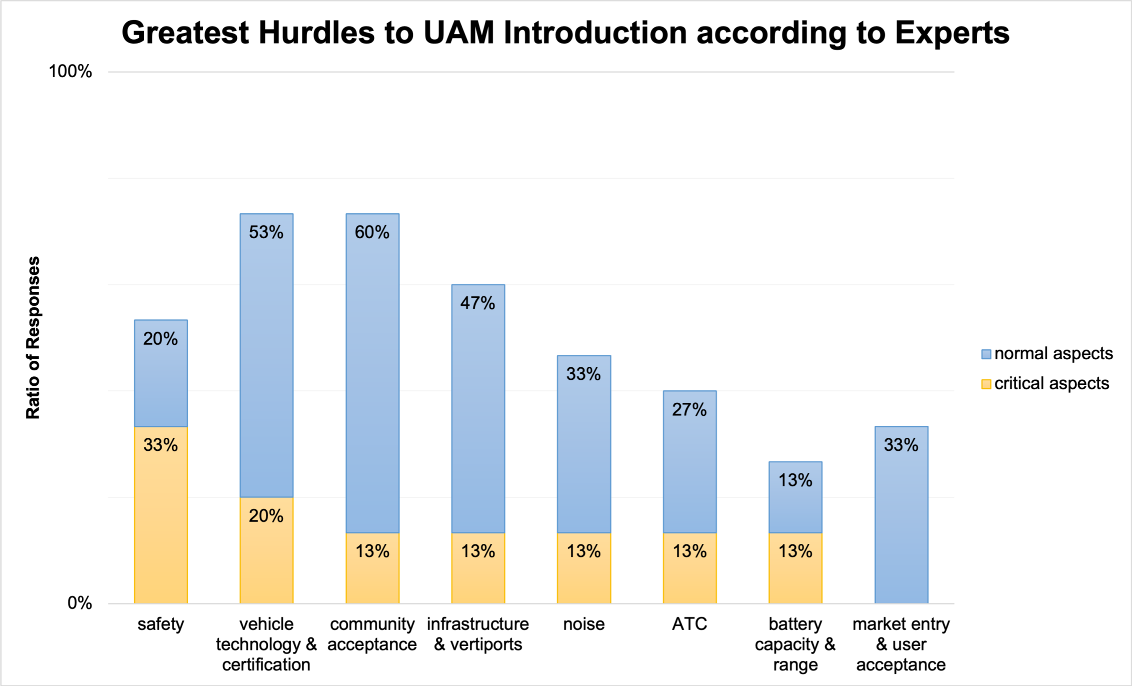

Figure 19: Responses of experts regarding definition, potentials, and hurdles of UAM.

4.2. Parameter determination (results)

After data analysis after each interview round, the resulting list of 24 parameters selected are shown in table 5. It includes a short, descriptive list and grouping of the final parameter list of 24 that is available to be used as new, refined inputs for the vertiport simulation.

Vertiport Elements
Dimensions of Pad
Dimensions of Gate
Dimensions of Stand
Dimensions of Taxiway

Passenger Processing Time
Passenger walking from holding place in terminal to gate

Passenger Boarding Time
Passenger board helicopter
Passenger deboard helicopter
Passenger leave gate
Passenger enter gate

Vehicle Taxiing
Speed of hover taxiing on Taxiway
Speed of passive taxiing device on Taxiway
Time to mount passive taxiing device
Time to demount passive taxiing device
Speed of active taxiing with motors at wheels

Takeoff and Landing Time
Starting Rotors
Stopping Rotors

Approach/Departure Flight Time
Initial hover
Final hover
Leaving Pad airspace
Entering Pad airspace
A/C separation

Battery Charging
Charging speed
Battery capacity of vehicle
Energy loss due to inefficiency

Table 5: List of final 24 parameters within respective groups.

There are several things to note related to the final parameter list of 24. The section *Vertiport Elements* refer to the parameter values that are related to vertiport infrastructure. In the section *Passenger Processing,* there was an original set of 6 parameters but it was decreased to only 1, the time it takes for a passenger to walk from holding place in terminal to gate. This parameter was determined to be the only critical passenger-related value in general vertiport operations, while other passenger processing parameters such as ticket scanning can be argued to also take place during e.g. boarding. The next section, *Passenger Boarding,* includes self-explanatory parameters related to the time it takes for passenger movement on and off the aircraft. *Vehicle Taxiing* is broken into two main distinctions: the speed of hover taxiing and the speed of passive taxiing. Hover taxiing refers to the technology that allows eVTOLs to hover just above ground to move the aircraft from pad to stand, and passive taxiing refers to the external devices attached to eVTOLs that push or pull the aircraft from one location the other. In *Takeoff and Landing,* the time it takes for vehicle rotors to start and stop are observed. Next, in the *Approach/Departure Flight Time,* the time of initial and final hover refers to how long it takes for the aircraft to leave and return to the airspace ground, respectively. *A/C separation* refers to the time separation minima between aircraft activities on the airfield. Lastly, the charging speed in *Battery Charging* specifies a speed with a non-constant effect in kilowatts, battery capacity in kilowatts per hour, and energy loss due to inefficiency in the form of the percentage of energy lost.

The following, table 6, shows the sum of responses per parameter received from experts in the first and second round of interviews.

Parameter	No. First Round	No. Second Round
Dimensions of Pad	1	1
Dimensions of Gate	0	1
Dimensions of Stand	0	1
Dimensions of Taxiway	0	1
Passenger walking from holding place in terminal gate	0	1
Passenger board helicopter	3	3
Passenger deboard helicopter	2	2
Passenger leave gate	0	1
Passenger enter gate	0	1
Speed of hover taxiing on Taxiway	0	2
Speed of passive taxiing device on Taxiway	4	2
Time to mount passive taxiing device	3	0
Time to demount passive taxiing device	3	0
Speed of active taxiing with motors at wheels	4	2
Starting Rotors	2	2
Stopping Rotors	2	1
Initial hover	3	2
Final hover	3	2
Leaving Pad airspace	3	1
Entering Pad airspace	3	1
A/C Separation	2	1
Charging speed	2	0
Battery capacity of vehicle	3	1
Energy loss due to inefficiency	2	0
Swapping Time	0	0

Table 6: Number of responses per parameter summed up in each interview round.

4.3. Deterministic modeling (results)

The final list including 63 experts responses and 53 literature datapoints (after applying weighted averaging from the methods section) with respective sources can be found in table 7. From this list, specific values were used in the final deterministic simulation. Some of the following deterministic parameters consists of only expert responses.

ID	Parameter	Unit	Final weighted average	Sources
A1	Dimensions of Pad	m	24.08	[59], [60], [61]
A3	Dimensions of Gate	m	27.43	[59], [60]
A5	Dimensions of Stand	m	30.00	
A7	Dimensions of Taxiway	m	21.78	[59], [60]
B11	Passenger walking from holding place in terminal gate	s	60.00	
C1	Passenger board helicopter	s	67.50	[62], [63], [60], [64], [12]
C4	Passenger deboard helicopter	s	60.95	[62], [63], [60], [12]
C5	Passenger leave gate	s	60.00	
C6	Passenger enter gate	s	60.00	
D2	Speed of hover taxiing on Taxiway	m/s	3.06	[65], [59], [60]
D4	Speed of passive taxiing device on Taxiway	m/s	2.06	
D5	Time to mount passive taxiing device	s	20.71	
D7	Time to demount passive taxiing device	s	20.71	
D8	Speed of active taxiing with motors at wheels	m/s	2.98	[66]
E1	Starting Rotors	s	4.67	
E2	Stopping Rotors	s	21.18	
F1	Initial hover	s	14.55	[67], [65], [68], [69], [44]
F2	Final hover	s	22.19	[67], [65], [68], [70]

ID	Parameter	Unit	Final weighted average	Sources
F3	Leaving Pad airspace	s	25.71	[69]
F4	Entering Pad airspace	s	34.53	[69], [12]
F11	A/C Separation	s	26.00	[71], [72], [73]
G3	Charging speed	kW	404.46	[74], [68], [75], [76], [66], [69]
G5	Battery capacity of vehicle	kWh	135.83	[67], [77]
G10	Energy loss due to inefficiency	%	7.60	[75], [69]

Table 7: List of literature and expert responses for final 24 parameters.

4.4. Stochastic modeling (results)

4.4.1. Skew distribution model outputs

The outputs from the Python script *create_factors* produced skew normal distribution curves for each expert response per parameter. Epsilon values per expert response and are printed in table 8. Parameters with epsilon values of -1 or 1 indicate expert responses that provided the value for expected as for minimum or maximum.

Expert	Parameter	Unit	Mu	Sigma	Epsilon
E1	C1	s	30.00	14.50	-0.17
E2	D4	m/s	2.78	1.04	-0.33
E2	D5	s	60.00	45.00	-0.33
E2	D7	s	60.00	45.00	-0.33
E2	D8	m/s	2.78	1.04	-0.33
E2	E2	s	60.00	22.50	-0.33
E3	D8	m/s	2.22	0.69	-0.40
E3	E1	s	5.00	1.17	-0.43
E3	E2	s	5.00	1.17	-0.43
E3	F1	s	30.00	15.00	-1.00
E3	F2	s	30.00	15.00	-1.00

Expert	Parameter	Unit	Mu	Sigma	Epsilon
E3	F3	s	60.00	60.00	-1.00
E3	F4	s	60.00	60.00	-1.00
E3	F11	s	30.00	20.00	-0.50
E3	G3	kW	300.00	125.00	-0.58
E3	G5	kWh	215.00	61.67	0.08
E4	C1	s	180.00	120.00	0.02
E4	C4	s	120.00	60.00	0.01
E4	F2	s	60.00	22.50	-0.33
E6	D4	m/s	1.00	0.17	-1.00
E6	D5	s	5.00	15.83	-1.00
E6	D7	s	5.00	15.83	-1.00
E7	D5	s	60.00	45.00	-0.33
E7	D7	s	60.00	45.00	-0.33
E7	D8	m/s	2.00	1.00	0.00
E7	G5	kWh	100.00	37.50	-0.33
E7	G10	%	3.00	1.00	0.00
E8	F1	s	5.00	0.75	-1.00
E8	F2	s	7.00	0.75	-1.00
E8	F3	s	5.00	0.50	-1.00
E8	F4	s	7.00	0.75	-1.00
E9	A1	m	15.00	1.50	-0.78
E9	C4	s	10.00	5.00	0.00
E9	D4	m/s	3.00	1.00	0.00
E9	F3	s	60.00	75.00	-0.59
E9	F4	s	60.00	75.00	-0.59
E10	G3	kW	150.00	75.00	-0.32

Expert	Parameter	Unit	Mu	Sigma	Epsilon
E10	G5	kWh	100.00	32.50	0.22
E10	G10	%	5.00	2.25	-0.11
E11	E1	s	3.00	4.00	-0.75
E11	E2	s	5.00	4.50	-0.11
E11	F1	s	2.00	2.00	-0.50
E11	F2	s	5.00	3.75	-0.33
E11	F3	s	3.00	2.00	0.00
E11	F4	s	3.00	2.00	0.00
E11	F11	s	10.00	13.50	-0.48
E12	G5	kWh	80.00	25.00	-0.19
E13	A1	m	50.00	17.50	-0.43
E13	A3	m	50.00	5.00	1.00
E13	A5	m	30.00	5.00	-1.00
E13	A7	m	30.00	5.00	-1.00
E13	C1	s	60.00	22.50	-0.33
E13	C4	s	60.00	22.50	-0.33
E13	D2	m/s	5.00	2.50	-1.00
E13	D4	m/s	2.50	0.63	-1.00
E13	F1	s	15.00	4.17	-0.20
E13	F2	s	15.00	4.17	-0.20
E14	B11	s	60.00	20.00	-0.50
E14	C5	s	60.00	20.00	-0.50
E14	C6	s	60.00	20.00	-0.50
E16	D2	m/s	7.22	1.39	0.20
E17	D8	m/s	4.47	0.60	-0.25

Table 8: Epsilon values created for each expert response per parameter.

4.4.2. Normal distribution model outputs

The Python script *aggregated_curves* produced skew normal distribution curves for each parameter according to each expert response. Outputs are displayed in figure 20.

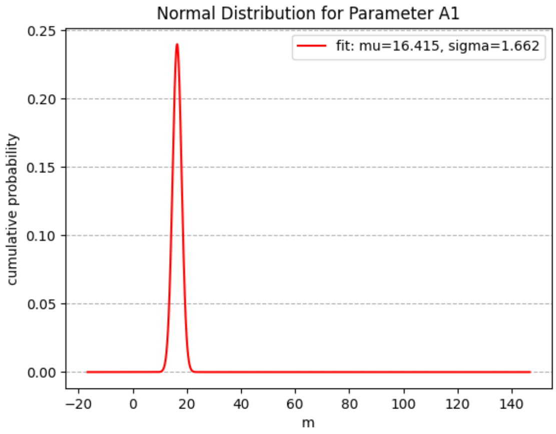
Normal Distribution for Parameter A1
fit: mu=16.415, sigma=1.662
cumulative probability
0.25
0.20
0.15
0.10
0.05
0.00
−20
0
20
40
60
80
100
120
140
m

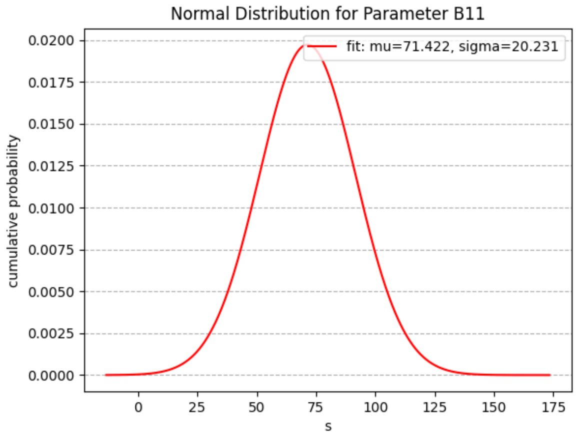
Normal Distribution for Parameter B11
fit: mu=71.422, sigma=20.231
cumulative probability
0.0200
0.0175
0.0150
0.0125
0.0100
0.0075
0.0050
0.0025
0.0000
0
25
50
75
100
125
150
175
s

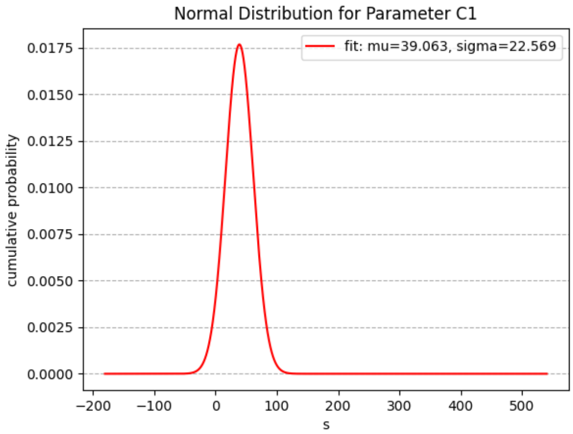
Normal Distribution for Parameter C1
fit: mu=39.063, sigma=22.569
cumulative probability
0.0175
0.0150
0.0125
0.0100
0.0075
0.0050
0.0025
0.0000
−200
−100
0
100
200
300
400
500
s

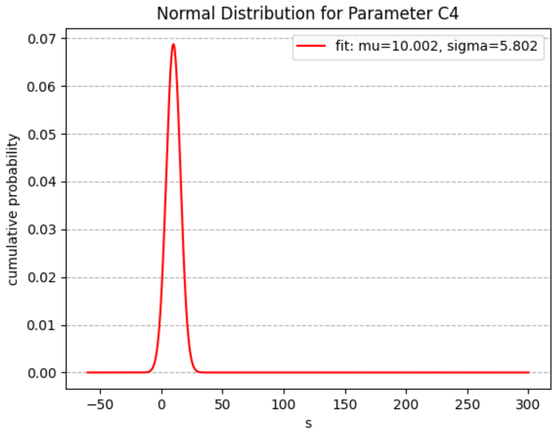
Normal Distribution for Parameter C4
fit: mu=10.002, sigma=5.802
cumulative probability
0.07
0.06
0.05
0.04
0.03
0.02
0.01
0.00
−50
0
50
100
150
200
250
300
s

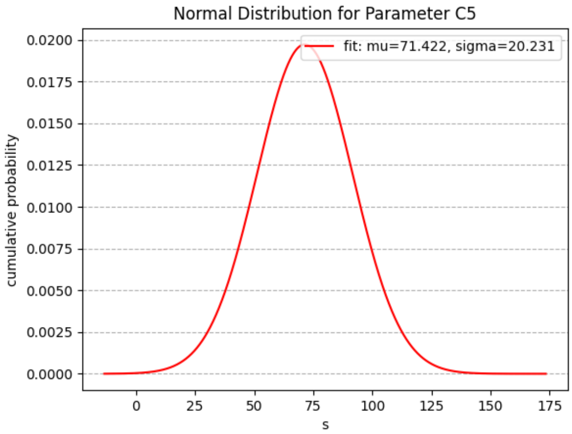
Normal Distribution for Parameter C5
fit: mu=71.422, sigma=20.231
cumulative probability
0.0200
0.0175
0.0150
0.0125
0.0100
0.0075
0.0050
0.0025
0.0000
0
25
50
75
100
125
150
175
s

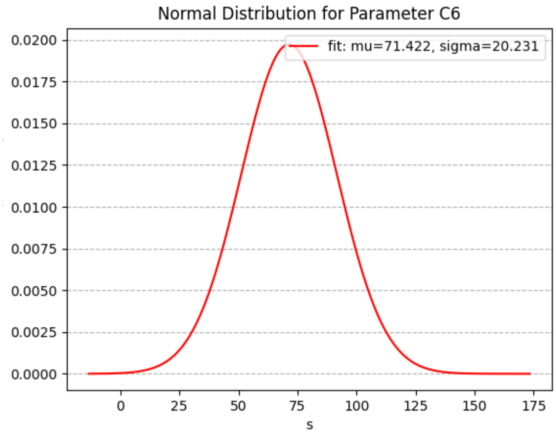
Normal Distribution for Parameter C6
fit: mu=71.422, sigma=20.231
0.0200
0.0175
0.0150
0.0125
0.0100
0.0075
0.0050
0.0025
0.0000
0
25
50
75
100
125
150
175
s

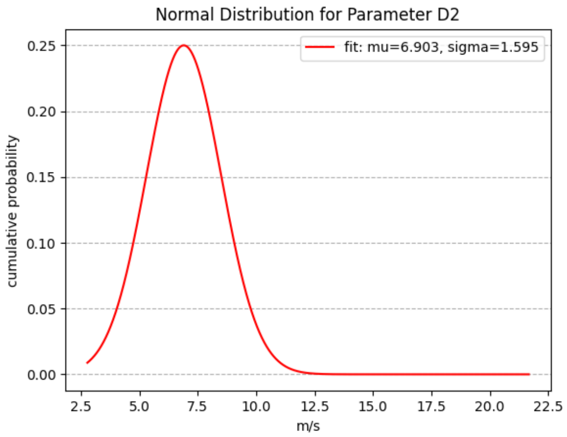
Normal Distribution for Parameter D2
fit: mu=6.903, sigma=1.595
cumulative probability
0.25
0.20
0.15
0.10
0.05
0.00
2.5
5.0
7.5
10.0
12.5
15.0
17.5
20.0
22.5
m/s

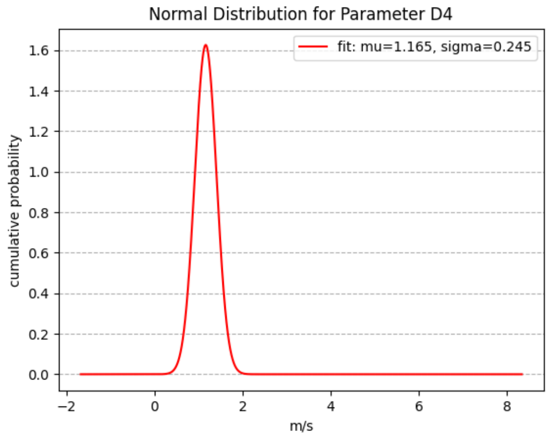
Normal Distribution for Parameter D4
fit: mu=1.165, sigma=0.245
cumulative probability
1.6
1.4
1.2
1.0
0.8
0.6
0.4
0.2
0.0
−2
0
2
4
6
8
m/s

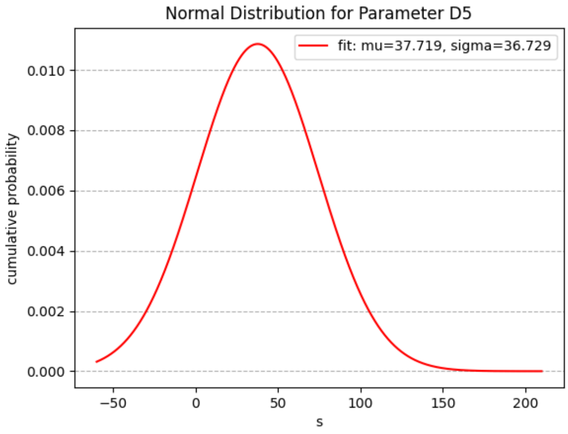
Normal Distribution for Parameter D5

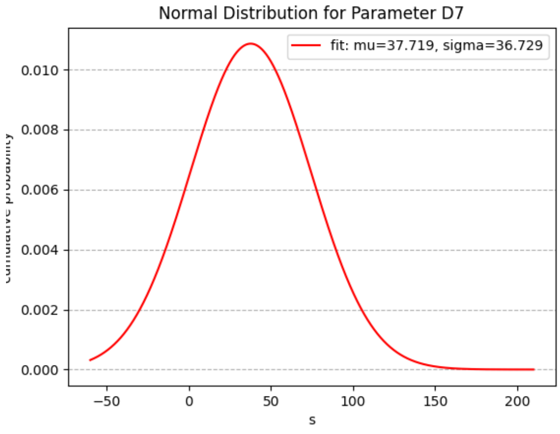
Normal Distribution for Parameter D7

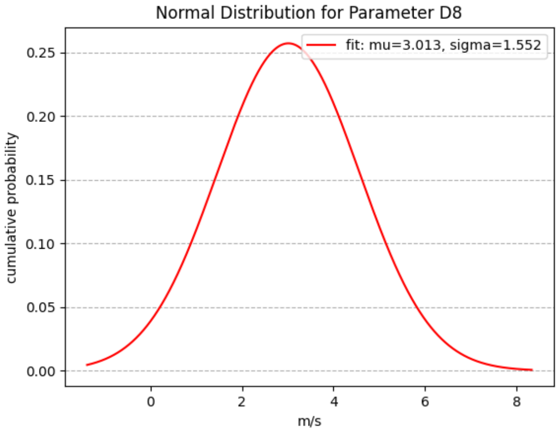
Normal Distribution for Parameter D8

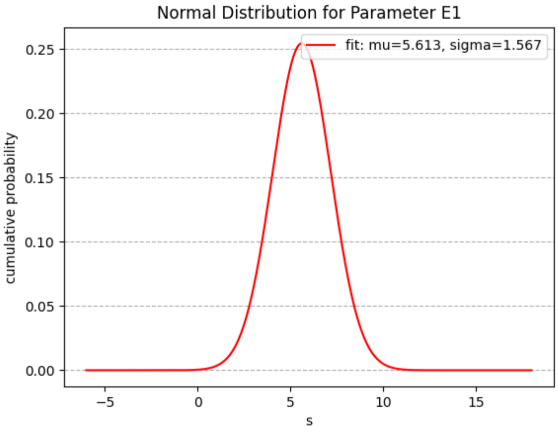
Normal Distribution for Parameter E1

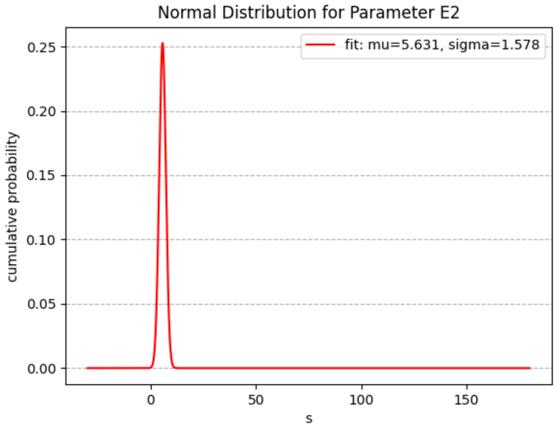
Normal Distribution for Parameter E2

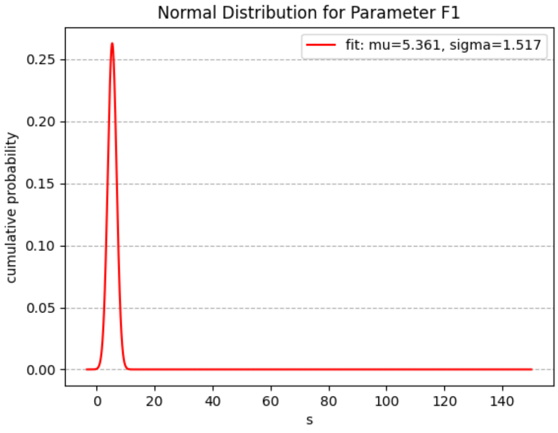
Normal Distribution for Parameter F1

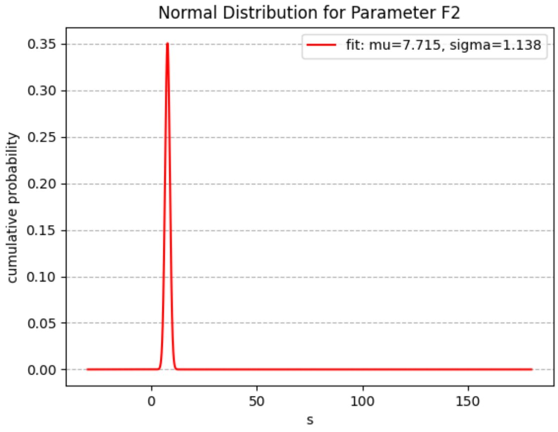
Normal Distribution for Parameter F2

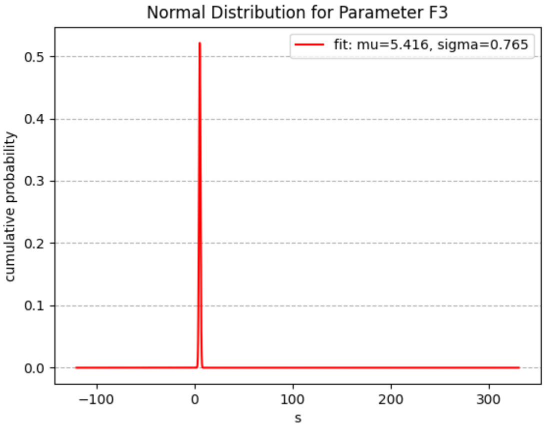
Normal Distribution for Parameter F3

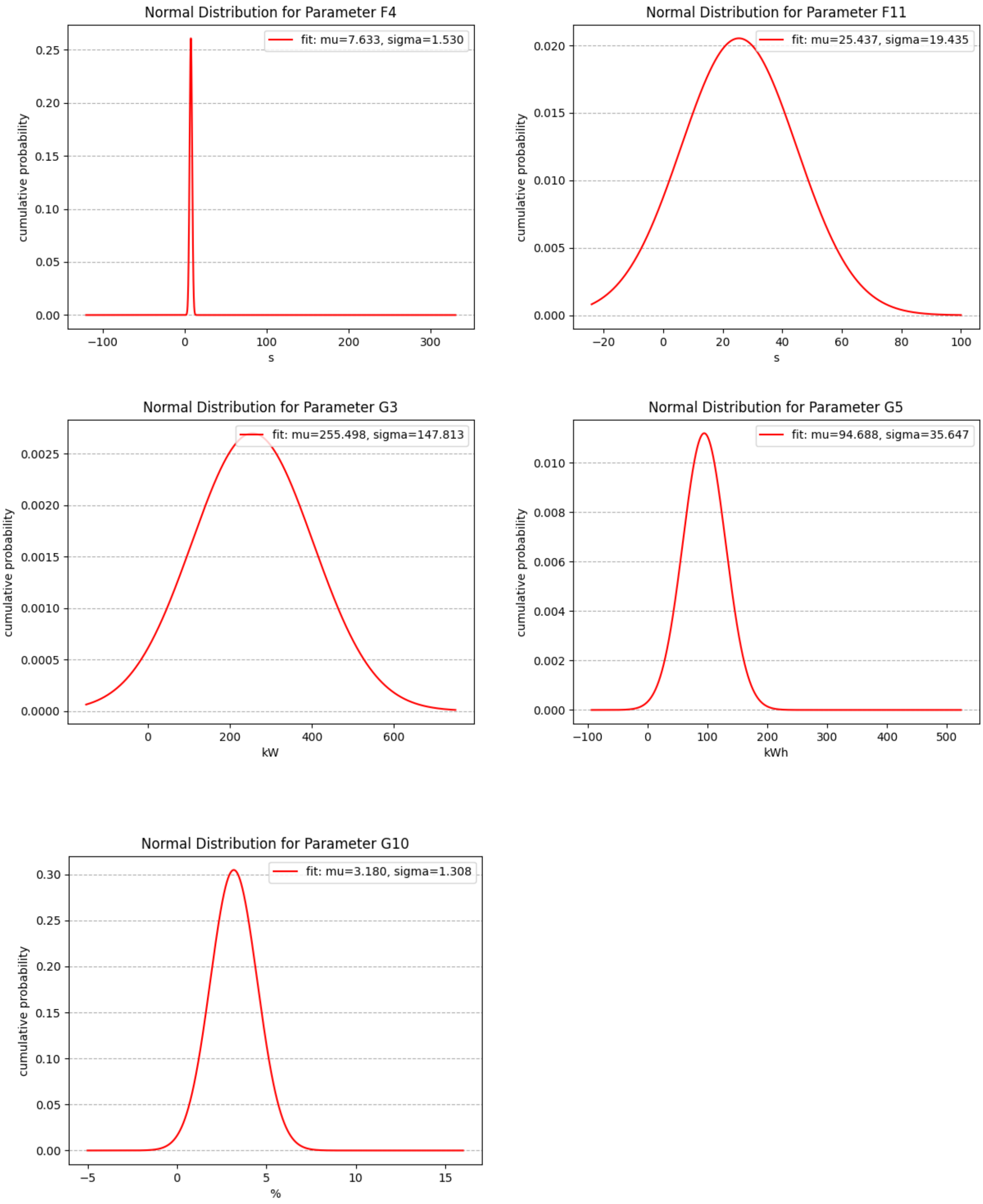

Figure 20: Normal distribution curves representing each parameter, classified by parameter IDs. As in Table 7, A1 is “Dimensions of Pad,” B11 is “Passenger walking from holding place in terminal gate,” C1 is “Passenger board helicopter,” C4 is “Passenger deboard helicopter,” C5 is “Passenger leave gate,” C6 is “Passenger enter gate,” D2 is “Speed of hover taxiing on Taxiway,” D4 is “Speed of passive taxiing device on Taxiway,” D5 is “Time to mount passive taxiing device,” D7 is “Time to demount passive taxiing device,” D8 is “Speed of active taxiing with motors at wheels,” E1 is “Starting Rotors,” E2

is “Stopping Rotors,” F1 is “Initial hover,” F2 is “Final hover,” F3 is “Leaving Pad airspace,” F4 is “Entering Pad airspace,” F11 is “A/C Separation,”G3 is “Charging speed,” G5 is “Battery capacity of vehicle,” and G10 is “Energy loss due to inefficiency.”

The graphs depicting aggregation from independent skew normal distributions per parameter are displayed in appendix 5. A3 “Dimensions of Gate,” A5 “Dimensions of Stand,” and A7 “Dimensions of Taxiway” are not shown because each parameter only has 1 response and whose minimum or maximum value equals the expected value. The skew normal distribution is therefore inaccurate and consequently disables Python’s ability to find a best normal curve fit in *aggregated_curves.*

4.5. Vertiport simulation

As described previously in section 3.4.3, the *population_generator* outputs of taxi speed, approach, departure, passenger walking time from terminal to gate, boarding time, and deboarding time were the inputs for Preis’ vertiport simulation. There were four scenarios conducted with the simulation, having the same starting population of 500 vehicles and 1000 passengers, and the same times between 6:00 and 22:00 but with other distinct inputs. Scenario A, *Baseline Deterministic,* uses default parameters from previous work as input for one run of the simulation. *Calibrated Deterministic,* scenario B, includes one run of the simulation parameter values derived from the weighted-average combination of expert responses and further literature review. Scenario C, *Baseline for Stochastic Variation,* uses only the expected “mu” value as parameter values in the simulation for one run of the simulation. Next, scenario D, *Stochastic Variation of Parameters,* consists of 5 simulation runs from input values generated through Monte Carlo random sampling. Lastly, scenario E, *Stochastic Variation of Time,* has 3 simulation runs in similar fashion as *Stochastic Variation of Parameters* but with randomly generated times between 6:00 and 22:00. For each scenario, the passenger waiting times, passenger states, vehicle states per hour of day, and occupancy states are shown for consistency in comaprison and analysis.

4.5.1. Scenario A: Baseline deterministic

The outputs of passenger waiting times, passenger states, and vehicle states per hour of the simulation are shown in figure 21.

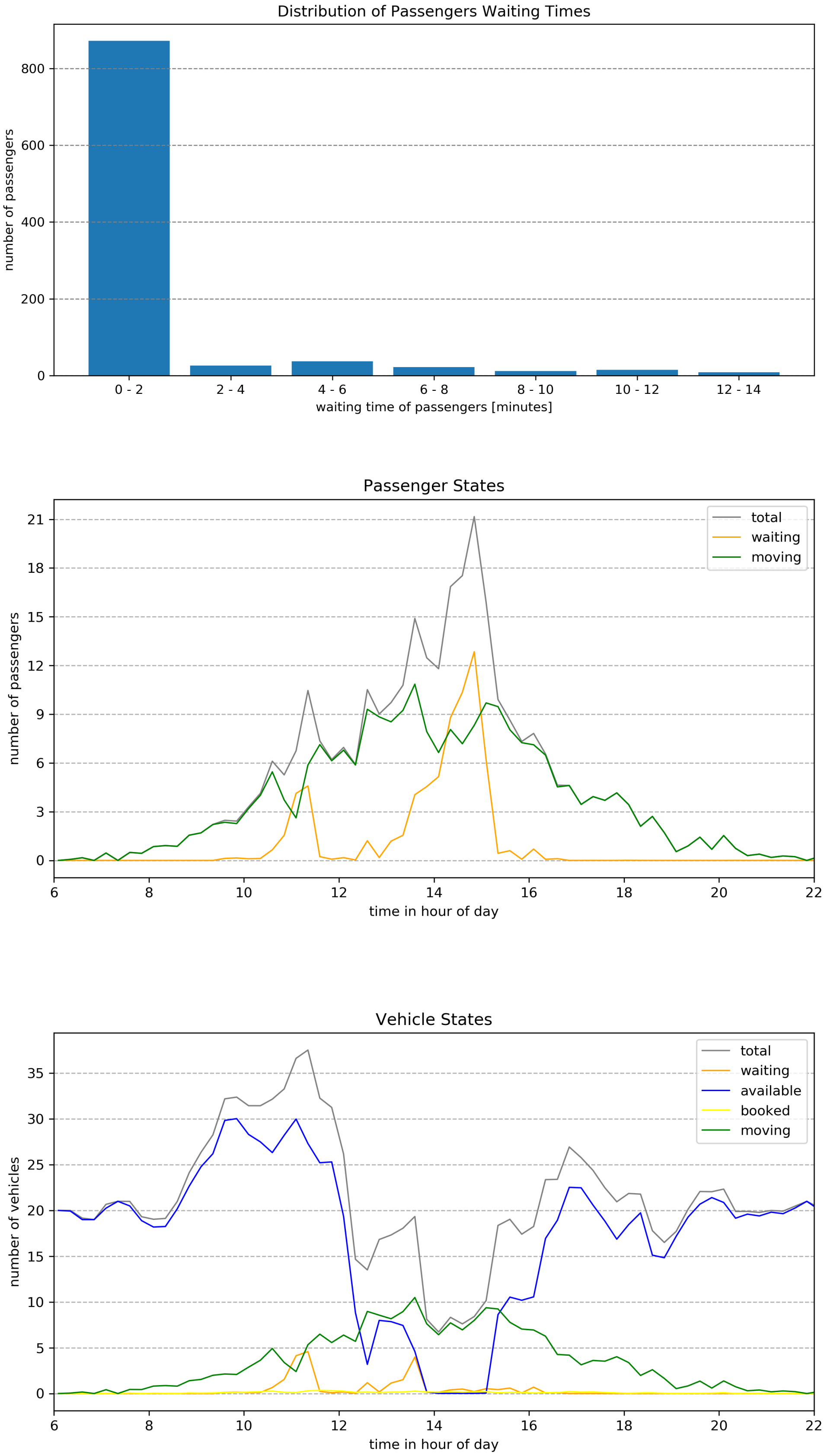

Figure 21: Distribution of passenger waiting times, passenger states, and vehicle states per hour of day for scenario A.

Below is the printout of summary of states throughout the simulation (table 9). As explained in figure 8, possible states for an element (pad, stand, or gate) is available and occupied, for a vehicle, available, busy, waiting, and occupied, and for a passenger, waiting and occupied.

Vehicle moving (%)	16.4
Passenger waiting (%)	22.6
Stand occupancy (%)	78.6
Pad occupancy (%)	25.7
Gate occupancy (%)	32.3

Table 9: Agent and element occupancy states for scenario A.

4.5.2. Scenario B: Calibrated deterministic

The outputs of passenger waiting times, passenger states, and vehicle states per hour of the simulation are shown in figure 22.

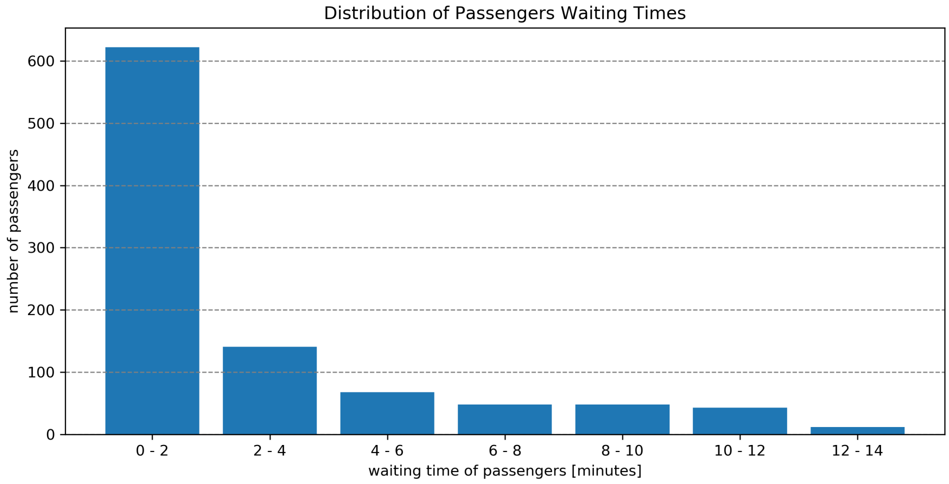

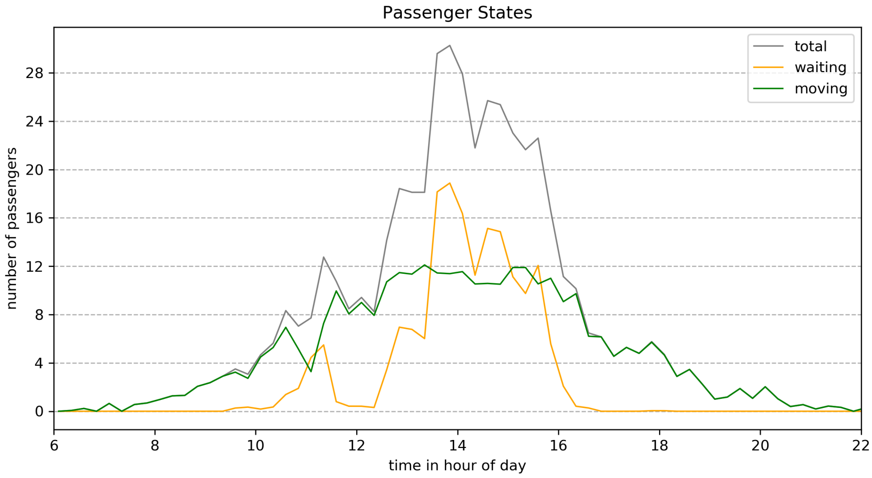

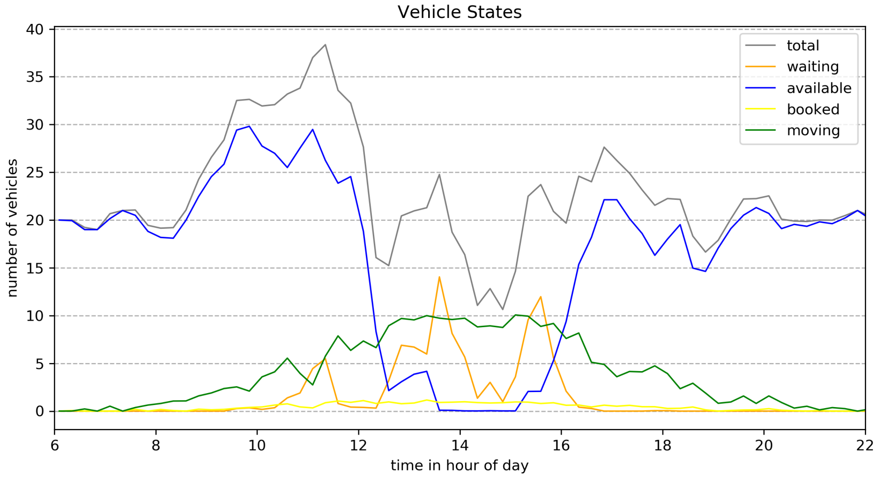

Figure 22: Passenger waiting times, passenger states, and vehicle states per hour of day for scenario B.

Accumulation of states for scenario B is shown in table 10.

Vehicle moving (%)	17.8
Passenger waiting (%)	35.5
Stand occupancy (%)	75.2
Pad occupancy (%)	37.7
Gate occupancy (%)	37.9

Table 10: Agent and element occupancy states for scenario B.

4.5.3. Scenario C: Baseline for stochastic variation

The outputs of passenger waiting times, passenger states, and vehicle states per hour of the simulation are shown in figure 23.

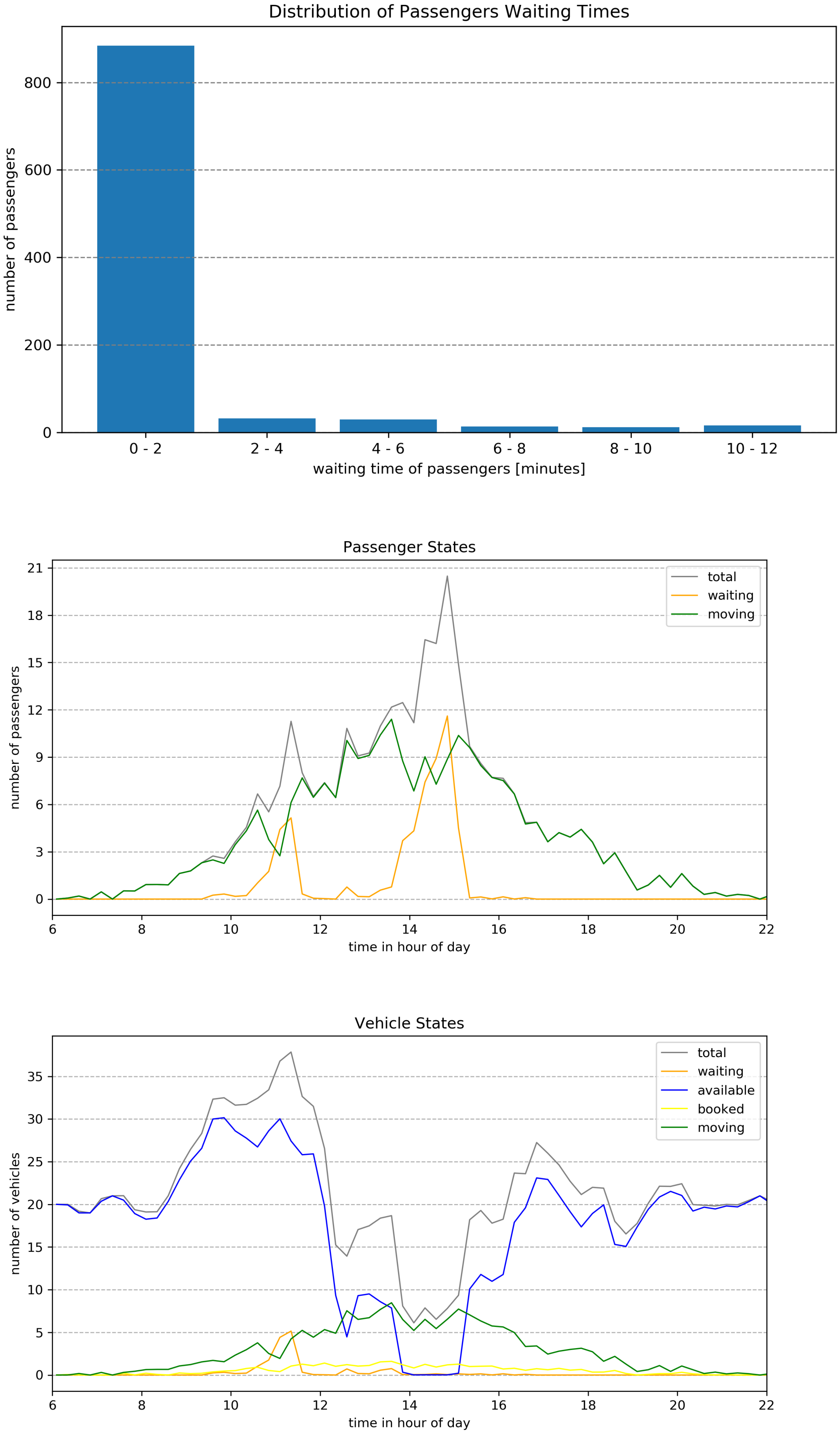

Figure 23: Passenger waiting times, passenger states, and vehicle states per hour of day for scenario C.

Accumulation of states for scenario C is shown in table 11.

Vehicle moving (%)	13.2
Passenger waiting (%)	18.3
Stand occupancy (%)	80.1
Pad occupancy (%)	19.1
Gate occupancy (%)	33.1

Table 11: Agent and element occupancy states for scenario C.

4.5.4. Scenario D: Stochastic variation of parameters

The 5 simulation runs of scenario D consists have very similar outputs and selected agent and element states between each run are highlighted in table 12. Thus, for the purposes of the future comparisons, only passenger waiting times, passenger states, and vehicle states per hour graphs from the first simulation run are shown (in figure 24).

	Run 1	**Run 2**	**Run 3**	**Run 4**	**Run 5**
Vehicle moving (%)	12.2	12.2	12.2	12.3	12.2
Passenger waiting (%)	18.1	18.3	18.0	18.2	18.2
Stand occupied (%)	80.2	80.1	80.2	80.2	80.2
Pad occupied (%)	20.2	20.4	20.1	19.7	19.8
Gate occupied (%)	33.3	33.4	33.5	33.5	33.6

Table 12: Selected agent and element states for 5 simulations runs of scenario D.

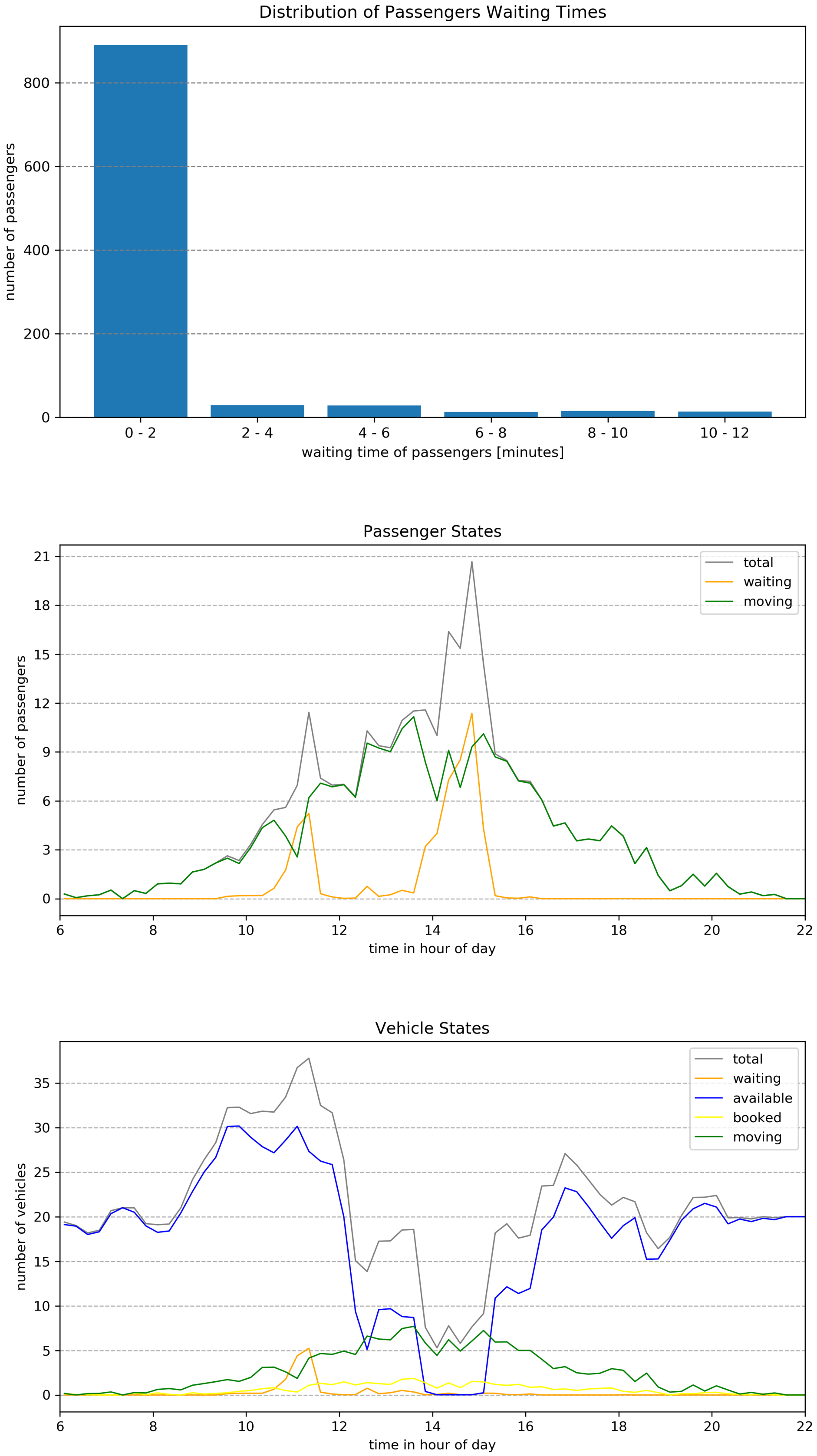

Figure 24: Passenger waiting times, passenger states, and vehicle states per hour of day for scenario D.

Accumulation of states for scenario D is shown in table 13.

Vehicle moving (%)	12.2
Passenger waiting (%)	18.1
Stand occupancy (%)	80.2
Pad occupancy (%)	20.2
Gate occupancy (%)	33.3

Table 13: Agent and element occupancy states for 1 run of scenario D.

4.5.5. Scenario E: Stochastic variation of times

Scenario E contains 3 simulation runs, between which there are distinguishable differences. Selected agent and element states between each run are highlighted these runs are captured in table 14. For simple illustrative purposes, only the outputs of 1 run are displayed in graphical form for passenger waiting times, passenger states, and vehicle states per hour graphs (figure 25).

	Run 1	**Run 2**	**Run 3**
Vehicle moving (%)	10.5	10.8	11.5
Passenger waiting (%)	2.5	6.5	3.4
Stand occupancy (%)	96.5	92.5	90.8
Pad occupancy (%)	19.9	19.8	20.2
Gate occupancy (%)	35.5	34.0	28.9

Table 14: Selected agent and element states for 3 simulations runs of scenario E.

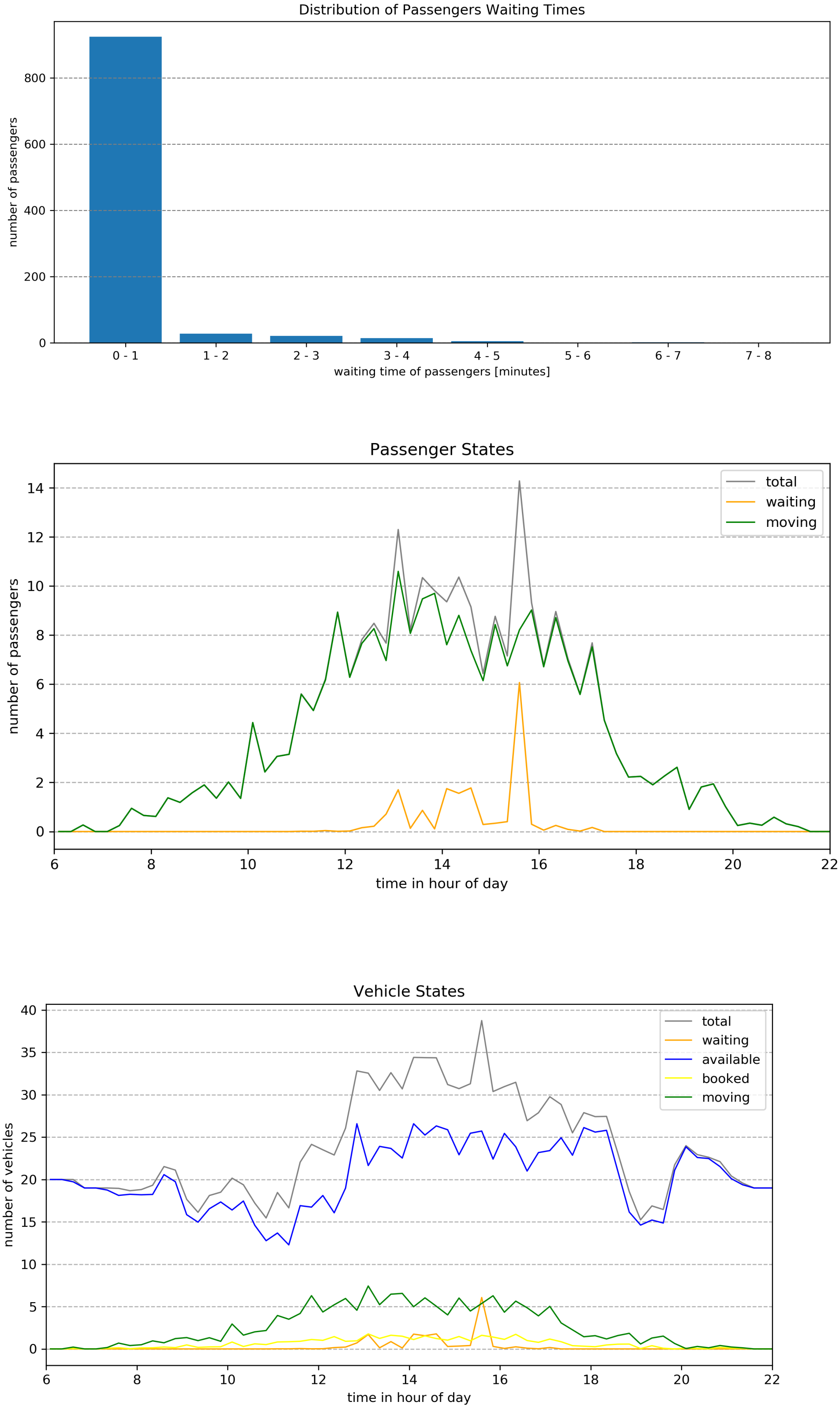

Figure 25: Passenger waiting times, passenger states, and vehicle states per hour of day for scenario E.

Accumulation of states for scenario C is shown in table 15.

Vehicle moving (%)	10.8
Passenger waiting (%)	6.5
Stand occupancy (%)	92.5
Pad occupancy (%)	19.8
Gate occupancy (%)	34.0

Table 15: Agent and element occupancy states for 1 run of scenario E.

5. Discussion

To validate the deterministic model and verify the vertiport model, comparisons between critical scenarios are performed. Focus of the analysis will be firstly based on the comparison between scenario A and B, scenario C and D, and scenario D and E. The research objective in the first comparison is to portray the effect of calibrated parameters of deterministic inputs, and the focus in the second and third comparisons is to determine the necessity of a stochastic model in calibrating inputs for the vertiport simulation.

5.1. Deterministic modeling (discussion)

Scenario A observes vertiport operational behavior according to the “baseline deterministic” model, which used default parameter values from previous work as inputs. Scenario B is the “calibrated deterministic” model and uses parameter values that were the averaged aggregation of experts’ estimated average values and further literature research findings.

5.1.1. Comparison of scenarios A and B

The following are some expectations of results based on the inputs:

- Higher values for approach and departure times increase vehicle occupancy.
- Higher values for passenger processing time (walking time from gate to terminal, boarding, and deboarding times) increases passenger waiting times.

Scenario B has higher approach and departure times as well as passenger processing times than scenario A, so it is assumed that scenario B would have higher vehicle occupancy and passenger waiting times. The results correctly demonstrate the anticipated behavior. Upon first glance of the graphs (figures 21 and 22), it can be observed that scenario B overall has more passengers waiting and generally more passengers in the simulation. Vehicle occupancy is observed to increase as there are approximately 9 vehicles moving during the busiest time in the simulation in scenario B compared to approximately 7 vehicles moving in scenario A (confirmed by an 8% increase in overall vehicle moving time). Furthermore, while around 12 passengers are in a waiting state at the simulation’s peak hour in scenario A, approximately 18 passengers are waiting during peak hour in scenario B. However, operational capacity increased in scenario B as there are more total passengers during peak hour as in scenario A, and approximately 25% less passengers wait between 0-2 minutes in scenario B than in scenario

A. Thus, it is concluded that both expectations are met and that overall occupancy of vertiport elements increased by 14% (tables 9 and 10).

Scenario B succeeded in using calibrated input parameter values to observe critical effects in vertiport operations and provide sensible insight to the simulation. While it is definitely worthwhile to conduct more trials similar to this comparison to gain greater insight, this achieves the goal of both validating the deterministic model and verifying the vertiport model.

5.2. Stochastic modeling (discussion)

Scenario C is the “baseline for stochastic variation” model, which uses stochastically-derived expected parameter “mu” values as inputs, and scenario D is the “stochastic variation of parameters” model which consists of 5 simulation runs using Monte Carlo-randomized parameter values as inputs. Firstly, the 5 simulations of scenario D were compared between each other to learn about the effects of Monte Carlo simulations on normal distributions. The expected behavior is small differences between each simulation, as the Monte Carlo technique usually results in an even, randomized distribution. Through comparing the occupancy levels between the 5 simulations in scenario D, this hypothesis was proven correct (table 13). There is less than 1% difference in any of the agent waiting and element occupancy levels between any two of the runs in scenario D. Therefore, the first run will be used as a representative simulation of scenario D in the comparisons going forward.

5.2.1. Comparison of scenarios C and D

The following are some expectations of results based on the inputs:

- Very similar agent and element occupancy levels in both scenarios.
- Similar values for passenger processing times in both scenarios.

The assumptions are made due to the nature of Monte Carlo’s method of random sampling and the normal distribution curves. In the same way that runs between scenario D do not differ greatly, runs between C and D should not differ much either. This was proven to be true when observing the nearly identical-looking graphs (figures 23 and 24) and observing the occupancy outputs of both scenarios (tables 11 and 13). Between scenario C and first Monte Carlo run of scenario D, there is only a 2% increase in occupancy across vertiport element levels. Additionally, passenger waiting times decreased by 1% from scenario C to D, implying similar passenger processing times. Through observing the graph printouts from both scenarios, they look almost identical. Therefore, it is concluded that scenarios C and D produce similar results.

In answering the research objective of determining the impact of stochastically-generated input parameters in the simulation, **the conclusion is that the stochastic model with only parameter variation does not provide new information on vertiport operational behavior and is therefore unnecessary.** However, this observation can also be due to the fact that agents did not really interact with each other since capacity was not reached. Another reason could be that both scenarios used the same times, so distributions of agents and availability of elements are nearly identical. Therefore, it is useful to perform another comparison between scenario D and scenario E, which has varied times, to comment on the impact of stochastic modeling for determining vertiport operational behavior in this simulation.

5.2.2. Comparison of scenarios D and E

Scenario E represents a time-varied version of scenario D. However, whereas scenario D has 5 simulation runs, scenario E has only 3 runs. In these 3 simulation runs, the objective is to observe whether or not a difference in time plans changes the vertiport's operational behavior. The occupancy levels between the 3 simulations in scenario E experience little variation, within 1% for pad occupancy and within 7% for stand and gate occupancy. However, there could be value in generating more simulations with varied times to analyze the general trend of element occupancy. Additionally, passenger waiting times fluctuate within a difference of 4%. These differences serve as a necessary background for the comparison between scenario D and scenario E and underline the effects of varied times on stochastic modeling for vertiport operations.

The following are some expectations of results between scenario D and E:

- They have similar global behavior and different local behavior for:
  - Element occupancy levels
  - Passenger processing times

Due to having the same inputs and only differing in time distributions, this comparison is expected to have varied arrivals and departure characteristics yet similar overall behavior. When first looking at the graphs of scenarios D and E, there are similar global trends in the passenger waiting times and passenger states graph, and different global trends in the vehicle states (figures 24 and 25). This points to the conclusion that passenger processing times differ globally. Additionally, through comparing and contrasting the occupancy outputs of both scenarios (tables 13 and 15), it can be concluded that the first assumption holds while the second is refuted. Compared to scenario D, element occupancy levels increased by a margin of 4% but passenger waiting time decreased by 64% in scenario E. However, it is interesting to note that while there are approximately 900 passengers who experience a waiting time between 0-2 minutes in scenario D, that range is 0-1 minute in scenario E. Also, in scenario D, there is a higher number of total passengers while in scenario E, there are less but more peak time intervals throughout the day. For vehicle occupancy, scenario D produces an hour where no vehicles are available while in scenario E, there are vehicles available at any given hour. Given all these differing characteristics, it seems that global behavior between the graphs display similar trends while their local behaviors vastly differ.

As there are quite a few differences in the occupancy levels and passenger processing behaviors, scenario E offers new insight on vertiport operations due to varying time distributions from scenario D. Since scenario E contains 3 simulation runs, it would be worthwhile to conduct further trials to gather more observations to draw more developed results. However, within the limitation of this study, **the conclusion is that a stochastic model with varying times is useful in providing a greater, critical understanding of the vertiport model and is therefore necessary in generating an accurate portrayal of vertiport operational behavior.**

6. Summary

The purpose of this thesis is to extend an existing vertiport model by calibrating input parameters through stochastic extensions and observing the effects in the simulated operations. Along with an introduction of “Urban Air Mobility” (UAM), it was illustrated in the state-of-the-arts section that emerging technologies for advanced transportation is important for urban development and environmental health. As such, the subject of UAM became increasingly scrutinized and UAM infrastructure was discovered to be a critical factor in actualizing its operations. Literature deemed this area of research to be lacking and consequently an increased interest in this topic was recently developed. This particular study extends Preis’ agent-based vertiport simulation framework, a Python model which simulates vertiport ground operations using input parameters related to vertiport operations. In order to calibrate input parameters, scientific interviews were organized in which experts from relevant industries were asked to provide their knowledge about UAM and give recommendations for the vertiport model. Experts were also asked to prepare estimations of critical operational parameters through giving minimum, expected, and maximum values as well as the confidence of their answers for each parameter. These responses were then used to create both a deterministic and stochastic model for generating calibrated input values. Through the iterative interview process, an original list of 82 parameters from previous work was also condensed to a list of 24 critical parameters to be considered in the deterministic and stochastic models.

The deterministic model was created through a weighted averaging method of values obtained through literature and experts’ estimated expected values. Furthermore, the stochastic model was derived from mathematical concepts of normal distribution and skew normal distribution. To achieve this, Python scripts were written to model the expert responses in skew normal distributions, and then to aggregate responses per parameter into normal distributions. The output was then further processed by using Monte Carlo simulations to be prepared into input files for the vertiport simulation.

Results from the vertiport simulation suggest that a calibrated deterministic model is necessary as it validates the model and verifies the vertiport simulation. It is also discovered that the stochastic model with varying parameter and time inputs provides more insight into the behavior of vertiport operations than that with only varying parameter inputs. Therefore, both the deterministic model and varied-time stochastic model achieved the purpose of this study to provide calibrated inputs as an extension for the vertiport simulation framework.

7. Future Work

Throughout this study, there were various limitations noted. An obvious constraint is the number of experts interviewed, their fields of expertise, and the selection of parameter values available in online scientific literature. Since experts in this study were drawn from personal connections, community networks, or social media such as LinkedIn, interviewed experts were limited to only those who responded to an invitation for interview. Specifically, the parameter value “battery swapping” was not able to be provided from this study’s interview series. As UAM is a dynamic field, another limiting factor were experts who were unwilling or disallowed to participate due to non-disclosure agreements with their companies. Future research can consider interviewing a higher number of experts from more varied academic backgrounds to gather more information and increase the quality of data obtained.

Operational parameters are the main inputs the vertiport model uses to simulate the behavior of ground operations. Therefore, as the vertiport simulation framework develops further and expands to reflect more operational behaviors, there is also the need to expand the list of critical parameters in vertiport operations and consequently the list of parameter inputs into the simulation.

The methods used to create the deterministic and stochastic models are limited in portraying data in their unique, specific ways. Therefore, there is value in applying different methods to establish both kinds of models through other mathematical means to arrive at different representations of data. Comparing result from different forms of data processing can afford new perspectives on data distribution and, consequently, different stochastic derivations of data used as inputs of the vertiport simulation.

It is also recommended for future work to perform more simulation runs of the scenarios, especially scenario E, to gather more observations. To reiterate, the purpose of scenario E was to understand the effects of varied times on stochastic modeling. While scenario A-D seem to attribute similar characteristics within the runs of each respective scenarios, scenario E displayed varied behavior in vertiport operations. Therefore, more runs would increase the quality of analysis thereafter. Additionally, there could be various new scenarios such as ones where there are both varied times and input parameters across the different scenarios to discover new operational effects and behaviors of the simulated vertiport.

References

[1] “Lilium closes $240M financing round for jet-like VTOL,” *electrive.com*, Mar. 23, 2020. https://www.electrive.com/2020/03/23/lilium-closes-financing-round-with-240-million/ (accessed Oct. 19, 2021).

[2] “Volocopter raises $55M led by Volvo owner Geely, sets 3-year timeline for its flying taxi service,” *TechCrunch*. https://social.techcrunch.com/2019/09/08/volocopter-raises-55m-led-by-volvo-owner-geely-sets-3-year-timeline-for-its-flying-taxi-service/ (accessed Oct. 19, 2021).

[3] T. Maxwell, “Uber partners with Joby Aviation for its air taxi service,” *Input*. https://www.inputmag.com/tech/uber-partners-with-joby-aviation-for-its-air-taxi-service (accessed Oct. 04, 2021).

[4] “What it takes to design an aircraft from scratch - Lilium.” https://lilium.com/newsroom-detail/lilium-architecture-design-principles (accessed Oct. 04, 2021).

[5] “Battery Swapping: Rückkehr der Austausch-Batterien?,” *InsideEVs Deutschland*. https://insideevs.de/news/489233/austauschbare-batterien-swap-china-ebikes-nio/ (accessed Oct. 04, 2021).

[6] P. D. Vascik and R. J. Hansman, “Development of Vertiport Capacity Envelopes and Analysis of Their Sensitivity to Topological and Operational Factors,” Jan. 2019, Accessed: Aug. 23, 2021. [Online]. Available: https://dspace.mit.edu/handle/1721.1/119874

[7] “VoloPort,” *Volocopter*. https://www.volocopter.com/solutions/voloport/ (accessed Oct. 19, 2021).

[8] L. Preis, A. Amirzada, and M. Hornung, “Ground Operation on Vertiports - Introduction of an Agent-Based Simulation Framework,” Jan. 2021. doi: 10.2514/6.2021-1898.

[9] B. Wang, W. Shi, and Z. Miao, “Confidence Analysis of Standard Deviational Ellipse and Its Extension into Higher Dimensional Euclidean Space,” *PloS One*, vol. 10, p. e0118537, Mar. 2015, doi: 10.1371/journal.pone.0118537.

[10] “Urban population set to increase by almost 700 million by 2030,” *Federal Statistical Office*. https://www.destatis.de/EN/Themes/Countries-Regions/International-Statistics/Data-Topic/Population-Labour-Social-Issues/DemographyMigration/UrbanPopulation.html (accessed Sep. 03, 2021).

[11] “The future of mobility 2020 | McKinsey.” https://www.mckinsey.com/industries/automotive-and-assembly/our-insights/the-future-of-mobility-is-at-our-doorstep (accessed Sep. 03, 2021).

[12] “Uber Elevate White Paper (Oct 2016).” https://evtol.news/news/uber-elevate-white-paper-oct-2016 (accessed Aug. 18, 2021).

[13] “UAM Concept of Operations (FAA),” Federal Aviation Administration NextGen, Jun. 2020. [Online]. Available: https://nari.arc.nasa.gov/sites/default/files/attachments/UAM_ConOps_v1.0.pdf

[14] L. Preis, *Concept of Operations for Urban Air Mobility: A Generic Development Approach*. 2020.

[15] R. Lineberger, A. Hussain, M. Metcalfe, and V. Rutgers, “Infrastructure barriers to the elevated future of mobility,” p. 14, 2019.

[16] R. Goyal *et al.*, “UAM Market Study (Booz Allen),” HQ-E-DAA-TN65181, Nov. 2018. Accessed: Aug. 23, 2021. [Online]. Available: https://ntrs.nasa.gov/citations/20190001472

[17] D. P. Thipphavong *et al.*, “Urban Air Mobility Airspace Integration Concepts and Considerations,” presented at the 2018 Aviation Technology, Integration, and Operations Conference, Atlanta, Georgia, Jun. 2018. doi: 10.2514/6.2018-3676.

[18] “Urban Air Mobility and Advanced Air Mobility.” https://www.faa.gov/uas/advanced_operations/urban_air_mobility/ (accessed Sep. 03, 2021).

[19] R. Rothfeld, M. Fu, M. Balac, and C. Antoniou, “Potential Urban Air Mobility Travel Time Savings: An Exploratory Analysis of Munich, Paris, and San Francisco,” *Sustainability*, vol. 13, p. 2217, Feb. 2021, doi: 10.3390/su13042217.

[20] A. Helland, “Well-to-wheel CO2 analysis of electric and ICE vehicles: are global CO2 emission reductions possible?,” *Int. J. Glob. Warm.*, vol. 1, no. 4, p. 432, 2009, doi: 10.1504/IJGW.2009.029214.

[21] “UAM Market Study NASA,” NASA Urban Air Mobility, Nov. 2018.

[22] “eVTOL Aircraft Complete Market Overview by TransportUP,” *TransportUP*. https://transportup.com/the-hangar/ (accessed Sep. 05, 2021).

[23] A. Bacchini and E. Cestino, “Electric VTOL Configurations Comparison,” *Aerospace*, vol. 6, p. 26, Feb. 2019, doi: 10.3390/aerospace6030026.

[24] G. Warwick, “eVTOL Certification: Who Are The Leaders? | Aviation Week Network.” https://aviationweek.com/aerospace/evtol-certification-who-are-leaders (accessed Sep. 05, 2021).

[25] “eVTOL Certification: Where Are They Now and the Challenges that Still Lie Ahead,” *Aviation Today*, May 24, 2021. https://www.aviationtoday.com/2021/05/24/evtol-certification-now-challenges-still-lie-ahead/ (accessed Sep. 05, 2021).

[26] “Helicopter booking service Blade goes public, with an eye toward future eVTOL ops,” *evtol.com*. https://evtol.com/news/helicopter-booking-service-blade-goes-public-eyeing-evtol-ops/ (accessed Sep. 07, 2021).

[27] “Acubed - Closing This Chapter: Our Learnings On Transforming How People Move.” https://acubed.airbus.com/blog/voom/closing-this-chapter-our-learnings-on-transforming-how-people-move/ (accessed Sep. 07, 2021).

[28] “Introducing Uber Copter | Uber Blog.” https://www.uber.com/blog/new-york-city/uber-copter/ (accessed Sep. 07, 2021).

[29] “Uber Elevate,” *Uber*. https://www.uber.com/us/en/elevate/ (accessed Sep. 07, 2021).

[30] “What is a VTOL aircraft? Definition from WhatIs.com.,” *WhatIs.com*. https://whatis.techtarget.com/definition/vertical-takeoff-and-landing-VTOL-aircraft (accessed Sep. 03, 2021).

[31] “Vertical Flight: How Things Fly,” n.d. https://howthingsfly.si.edu/propulsion/vertical-flight

[32] “Electric Taxiing Systems: Past, Present and the Possible Future,” *Aviation Today*, May 01, 2019. https://www.aviationtoday.com/2019/05/01/electric-taxiing-systems-past-present-possible-future/ (accessed Sep. 05, 2021).

[33] M. Lukic *et al.*, “State of the Art of Electric Taxiing Systems,” Nov. 2018. doi: 10.1109/ESARS-ITEC.2018.8607786.

[34] “Innovative TaxiBot now used in real flight operations | IAI.” https://www.iai.co.il/innovative-taxibot-now-used-real-flight-operations (accessed Sep. 05, 2021).

[35] “WheelTug Initiates Manufacturing Process – WheelTug.” https://www.wheeltug.com/?p=2362 (accessed Sep. 05, 2021).

[36] D. P. Nathen, D. A. Bardenhagen, D. A. Strohmayer, R. Miller, D. S. Grimshaw, and D. J. Taylor, “Architectural performance assessment of an electric vertical take-off and landing (e-VTOL) aircraft based on a ducted vectored thrust concept,” p. 35, 2021.

[37] “EASA Study on the societal acceptance of Urban Air Mobility in Europe,” European Union Aviation Safety Agency, May 2021.

[38] F. Adegbohun, A. Jouanne, and K. Lee, “Autonomous Battery Swapping System and Methodologies of Electric Vehicles,” *Energies*, vol. 12, p. 667, Feb. 2019, doi: 10.3390/en12040667.

[39] J. Pettitt, “Why battery swapping may finally become a part of EV charging infrastructure in the U.S.,” *CNBC*, May 29, 2021. https://www.cnbc.com/2021/05/29/how-ample-is-bringing-battery-swapping-to-the-us.html (accessed Sep. 06, 2021).

[40]W. Hofer, “Nio launcht Akkutausch-Station der zweiten Generation,” *electrive.net*, Apr. 15, 2021. https://www.electrive.net/2021/04/15/nio-launcht-akkutausch-station-der-zweiten-generation/ (accessed Sep. 06, 2021).
[41]“Gone in 90 Seconds: Geely’s Solution to Vehicle Charging,” *Media Center - Zhejiang Geely Holding Group*. http://zgh.com/media-center/story/gone-in-90-seconds/?lang=en (accessed Sep. 06, 2021).
[42]“EV Charging Points Over Time | Electric Cars | NewMotion,” *EV Charging Points Over Time | Electric Cars | NewMotion*. https://newmotion.com/en-gb/knowledge-centre/news-and-updates/the-evolution-of-charging-stations (accessed Sep. 06, 2021).
[43]A. Hove and D. Sandalow, “ELECTRIC VEHICLE CHARGING IN CHINA AND THE UNITED STATES,” p. 88, Feb. 2019.
[44]A. Brown and W. L. Harris, “Vehicle Design and Optimization Model for Urban Air Mobility,” *J. Aircr.*, vol. 57, no. 6, pp. 1003–1013, Nov. 2020, doi: 10.2514/1.C035756.
[45]“Advisory Circular for Heliport Design,” Federal Aviation Administration, Apr. 2012.
[46]“Advisory Circular for Vertiport Design,” Federal Aviation Administration, May 1991.
[47]“Air Traffic Organization Policy,” Federal Aviation Administration, Dec. 2015.
[48]“NATA UAM White Paper,” National Air Transportation Association. Accessed: Aug. 23, 2021. [Online]. Available: https://www.nata.aero/assets/Site_18/files/GIA/NATA%20UAM%20White%20Paper%20-%20FINAL%20cb.pdf
[49]M. Daskilewicz, B. German, M. Warren, L. A. Garrow, S.-S. Boddupalli, and T. H. Douthat, “Progress in Vertiport Placement and Estimating Aircraft Range Requirements for eVTOL Daily Commuting,” in *2018 Aviation Technology, Integration, and Operations Conference*, American Institute of Aeronautics and Astronautics, 2018. doi: 10.2514/6.2018-2884.
[50]“VoloPort (Volocopter),” *Volocopter*. https://www.volocopter.com/solutions/voloport/ (accessed Sep. 07, 2021).
[51]“VoloPort (Skyport),” *Skyports*. https://skyports.net/projects/volo-port/ (accessed Sep. 07, 2021).
[52]“Building vertiport cities,” *Aerospace America*, Jul. 01, 2021. https://aerospaceamerica.aiaa.org/features/building-vertiport-cities/ (accessed Sep. 07, 2021).
[53]K. O. Ploetner *et al.*, “Long-term application potential of urban air mobility complementing public transport: an upper Bavaria example,” *CEAS Aeronaut. J.*, vol. 11, no. 4, pp. 991–1007, Dec. 2020, doi: 10.1007/s13272-020-00468-5.
[54]M. Meuser and U. Nagel, “ExpertInneninterviews — vielfach erprobt, wenig bedacht,” in *Das Experteninterview: Theorie, Methode, Anwendung*, A. Bogner, B. Littig, and W. Menz, Eds. Wiesbaden: VS Verlag für Sozialwissenschaften, 2002, pp. 71–93. doi: 10.1007/978-3-322-93270-9_3.
[55]A. Bogner, B. Littig, and W. Menz, *Interviewing Experts*. 2009.
[56]L. V. Audenhove, “Expert Interviews and Interview Techniques for Policy Analysis,” Vrije Universiteit Brussel, Sep. 05, 2007.
[57]A. Azzalini, “A Class of Distributions Which Includes the Normal Ones,” *Scand. J. Stat.*, vol. 12, no. 2, pp. 171–178, 1985.
[58]G. Mudholkar and A. Hutson, “The epsilon-skew-normal distribution for analyzing near-normal data,” *J. Stat. Plan. Inference*, vol. 83, pp. 291–309, Feb. 2000, doi: 10.1016/S0378-3758(99)00096-8.
[59]K. Schweiger, F. Knabe, and B. Korn, “An exemplary definition of a vertidrome’s airside concept of operations,” *Aerosp. Sci. Technol.*, p. 107144, Oct. 2021, doi: 10.1016/j.ast.2021.107144.
[60]S. Zelinski, “Operational Analysis of Vertiport Surface Topology,” in *2020 AIAA/IEEE 39th Digital Avionics Systems Conference (DASC)*, Oct. 2020, pp. 1–10. doi: 10.1109/DASC50938.2020.9256794.
[61]“The Roadmap to scalable Urban Air Mobility: White Paper 2.0,” Bruchsal, Germany, 2021. Accessed: May 03, 2021. [Online]. Available: https://

www.volocopter.com/content/uploads/20210324_Volocopter_WhitePaper_Roadmap_to_scalable_UAM_m.pdf

[62] N. M. Guerreiro, R. W. Butler, J. M. Maddalon, and G. E. Hagen, “Mission Planner Algorithm for Urban Air Mobility – Initial Performance Characterization,” in *AIAA Aviation 2019 Forum*, American Institute of Aeronautics and Astronautics. doi: 10.2514/6.2019-3626.

[63] N. M. Guerreiro, G. E. Hagen, J. M. Maddalon, and R. W. Butler, “Capacity and Throughput of Urban Air Mobility Vertiports with a First-Come, First-Served Vertiport Scheduling Algorithm,” in *AIAA AVIATION 2020 FORUM*, American Institute of Aeronautics and Astronautics. doi: 10.2514/6.2020-2903.

[64] “PAXelerate - An Open Source Passenger Flow Simulation Framework for Advanced Aircraft Cabin Layouts | 54th AIAA Aerospace Sciences Meeting,” *AIAA SciTech Forum*. https://arc.aiaa.org/doi/abs/10.2514/6.2016-1284 (accessed Oct. 20, 2021).

[65] R. F. Vitalle, Y. Zhang, B. Normann, and N. Shen, “A Model for the Integration of UAM operations in and near Terminal Areas,” in *AIAA AVIATION 2020 FORUM*, American Institute of Aeronautics and Astronautics. doi: 10.2514/6.2020-2864.

[66] “Uber Air Vehicle Requirements and Missions,” Uber. Accessed: Aug. 18, 2021. [Online]. Available: https://s3.amazonaws.com/uber-static/elevate/Summary+Mission+and+Requirements.pdf

[67] I. Chakraborty and A. A. Mishra, “Total Energy Based Flight Control System Design for a Lift-Plus-Cruise Urban Air Mobility Concept,” in *AIAA Scitech 2021 Forum*, American Institute of Aeronautics and Astronautics. doi: 10.2514/6.2021-1899.

[68] S. Roy *et al.*, “A Multi-Commodity Network Flow Approach for Optimal Flight Schedules for an Airport Shuttle Air Taxi Service,” in *AIAA Scitech 2020 Forum*, American Institute of Aeronautics and Astronautics. doi: 10.2514/6.2020-0975.

[69] L. W. Kohlman and M. D. Patterson, “System-Level Urban Air Mobility Transportation Modeling and Determination of Energy-Related Constraints,” in *2018 Aviation Technology, Integration, and Operations Conference*, American Institute of Aeronautics and Astronautics, 2018. doi: 10.2514/6.2018-3677.

[70] M. D. Patterson, K. R. Antcliff, and L. W. Kohlman, “A Proposed Approach to Studying Urban Air Mobility Missions Including an Initial Exploration of Mission Requirements,” presented at the Annual Forum and Technology Display, Phoenix, AZ, May 2018. Accessed: Aug. 18, 2021. [Online]. Available: https://ntrs.nasa.gov/citations/20190000991

[71] “Rolling-Horizon Electric Vertical Takeoff and Landing Arrival Scheduling for On-Demand Urban Air Mobility | Journal of Aerospace Information Systems.” https://arc.aiaa.org/doi/abs/10.2514/1.I010776 (accessed Oct. 20, 2021).

[72] A. Maheshwari, S. Mudumba, B. Sells, D. DeLaurentis, and W. Crossley, *Identifying and Analyzing Operations Limits for Passenger-Carrying Urban Air Mobility Missions*. 2020. doi: 10.2514/6.2020-2913.

[73] P. D. (Parker D. N. Vascik, “Systems analysis of urban air mobility operational scaling,” Thesis, Massachusetts Institute of Technology, 2020. Accessed: Oct. 20, 2021. [Online]. Available: https://dspace.mit.edu/handle/1721.1/128057

[74] W. Finkeldei, E. Feldhoff, and G. S. Roque, “Flughafen Köln/Bonn Flugtaxi Infrastruktur FKBFTI,” p. 135, Feb. 2020.

[75] C. Y. Justin, A. P. Payan, S. I. Briceno, B. J. German, and D. N. Mavris, “Power optimized battery swap and recharge strategies for electric aircraft operations,” *Transp. Res. Part C Emerg. Technol.*, vol. 115, p. 102605, Jun. 2020, doi: 10.1016/j.trc.2020.02.027.

[76] P. Stith and J. Khangura, “Preparing for Take-Off: Urban Air Mobility Infrastructure National Institute of Aerospace (NIA) National Aeronautics and Space Administration (NASA) Study Results,” presented at the EVS33, Sep. 13, 2020. doi: 10.5281/zenodo.4027893.

[77] H. Eißfeldt, “Sustainable Urban Air Mobility Supported with Participatory Noise Sensing,” *Sustainability*, vol. 12, no. 8, Art. no. 8, Jan. 2020, doi: 10.3390/su12083320.

Declaration

I hereby confirm that the presented thesis work has been done independently and using only the sources and resources as are listed. This thesis has not previously been submitted elsewhere for purposes of assessment.

Place, Date, Signature

Appendix

Appendix 1 displays the interview guide that was used by the 7 experts who participated in the second round of interviews.

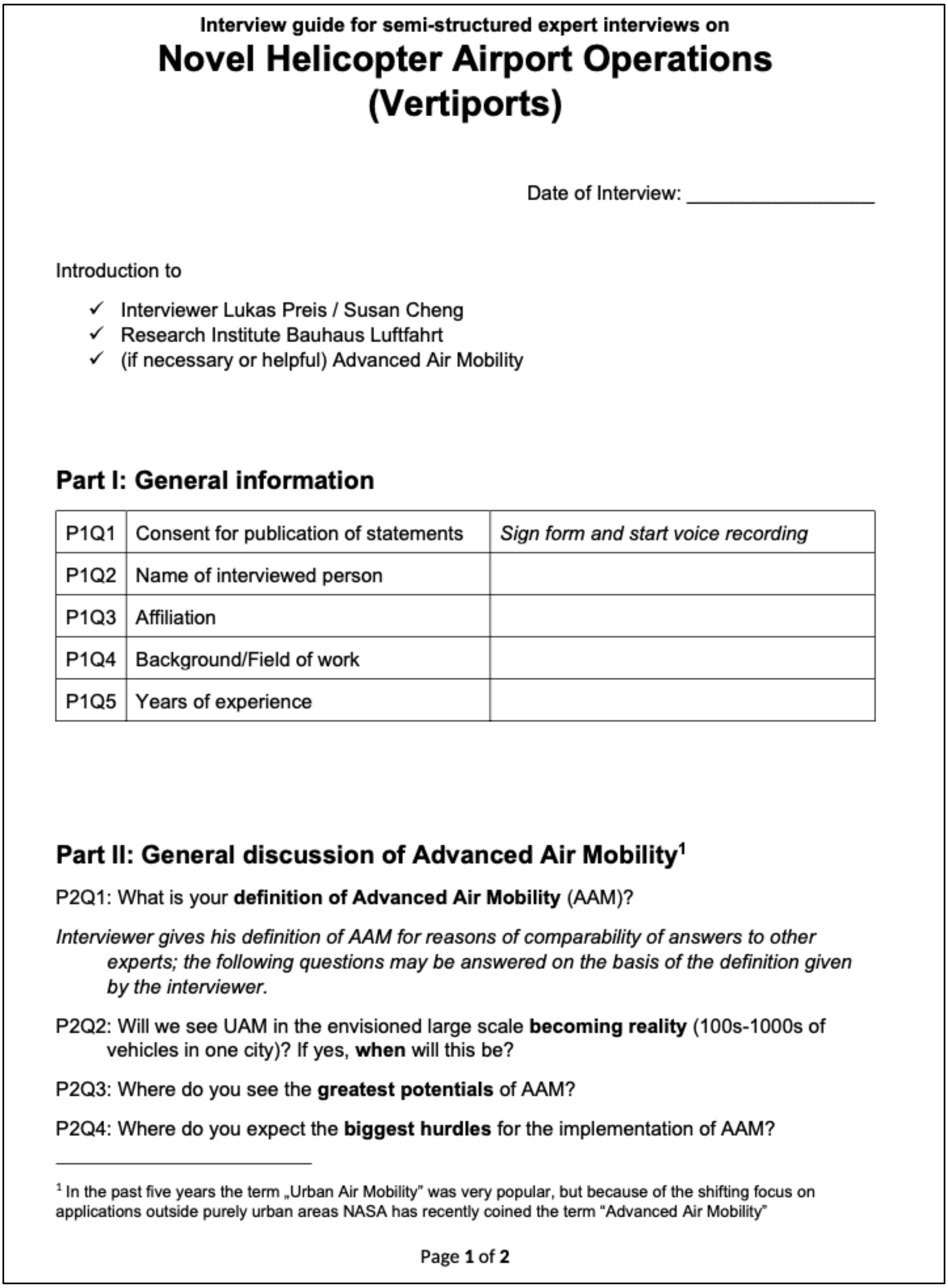

Interview guide for semi-structured expert interviews on

Novel Helicopter Airport Operations (Vertiports)

Date of Interview: __________________

Introduction to

- ✓ Interviewer Lukas Preis / Susan Cheng
- ✓ Research Institute Bauhaus Luftfahrt
- ✓ (if necessary or helpful) Advanced Air Mobility

Part I: General information

P1Q1	Consent for publication of statements	*Sign form and start voice recording*
P1Q2	Name of interviewed person	
P1Q3	Affiliation	
P1Q4	Background/Field of work	
P1Q5	Years of experience	

Part II: General discussion of Advanced Air Mobility[1]

P2Q1: What is your **definition of Advanced Air Mobility** (AAM)?

Interviewer gives his definition of AAM for reasons of comparability of answers to other experts; the following questions may be answered on the basis of the definition given by the interviewer.

P2Q2: Will we see UAM in the envisioned large scale **becoming reality** (100s-1000s of vehicles in one city)? If yes, **when** will this be?

P2Q3: Where do you see the **greatest potentials** of AAM?

P2Q4: Where do you expect the **biggest hurdles** for the implementation of AAM?

---

[1] In the past five years the term „Urban Air Mobility" was very popular, but because of the shifting focus on applications outside purely urban areas NASA has recently coined the term "Advanced Air Mobility"

Page **1** of **2**

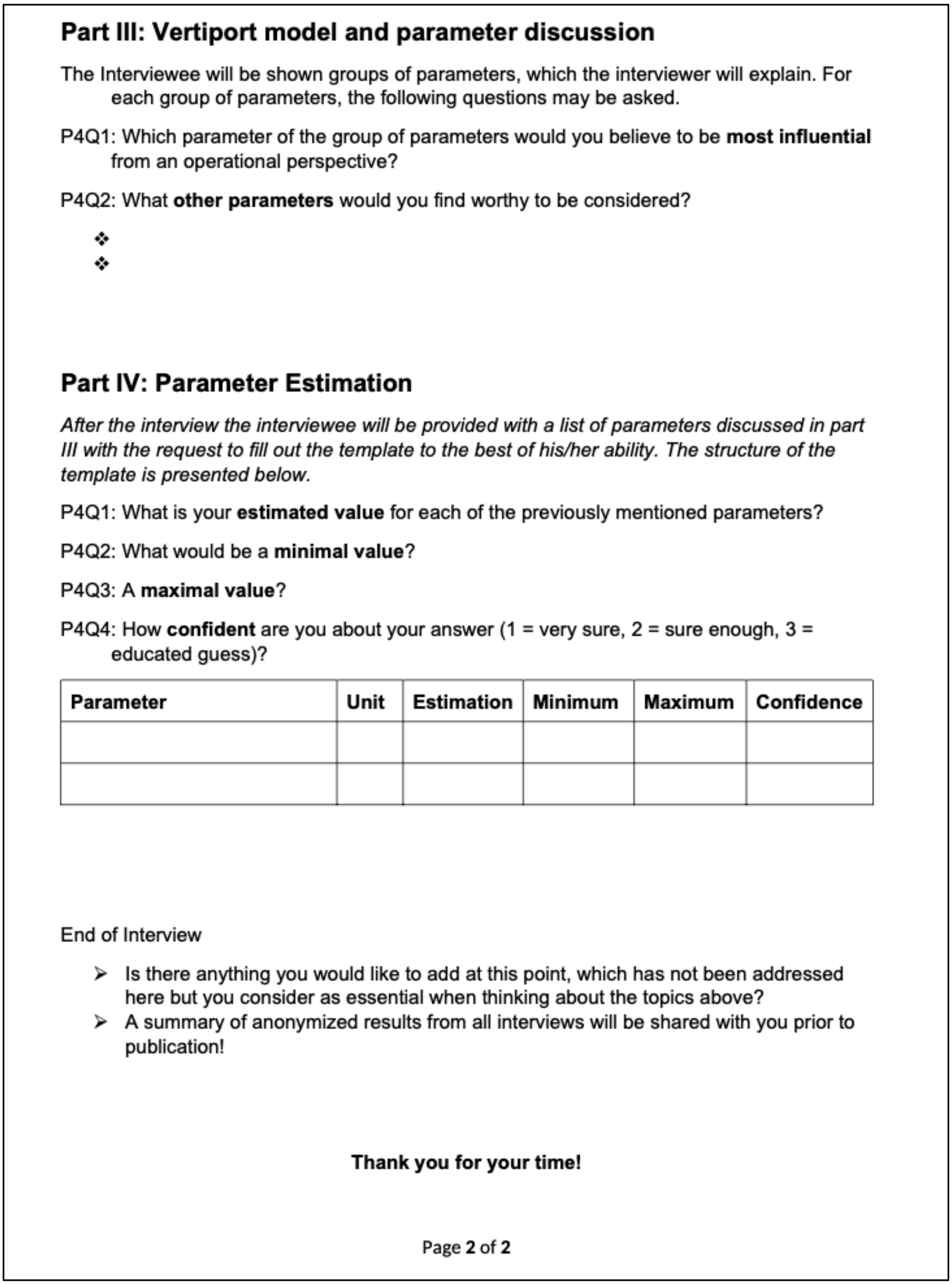

Part III: Vertiport model and parameter discussion

The Interviewee will be shown groups of parameters, which the interviewer will explain. For each group of parameters, the following questions may be asked.

P4Q1: Which parameter of the group of parameters would you believe to be **most influential** from an operational perspective?

P4Q2: What **other parameters** would you find worthy to be considered?

❖
❖

Part IV: Parameter Estimation

After the interview the interviewee will be provided with a list of parameters discussed in part III with the request to fill out the template to the best of his/her ability. The structure of the template is presented below.

P4Q1: What is your **estimated value** for each of the previously mentioned parameters?

P4Q2: What would be a **minimal value**?

P4Q3: A **maximal value**?

P4Q4: How **confident** are you about your answer (1 = very sure, 2 = sure enough, 3 = educated guess)?

Parameter	Unit	Estimation	Minimum	Maximum	Confidence

End of Interview

- Is there anything you would like to add at this point, which has not been addressed here but you consider as essential when thinking about the topics above?
- A summary of anonymized results from all interviews will be shared with you prior to publication!

Thank you for your time!

Appendix 1: Expert interview guide in second round.

Appendix 2 presents the groups of parameters related to vertiport operations that were introduced to the experts in the second round of interviews.

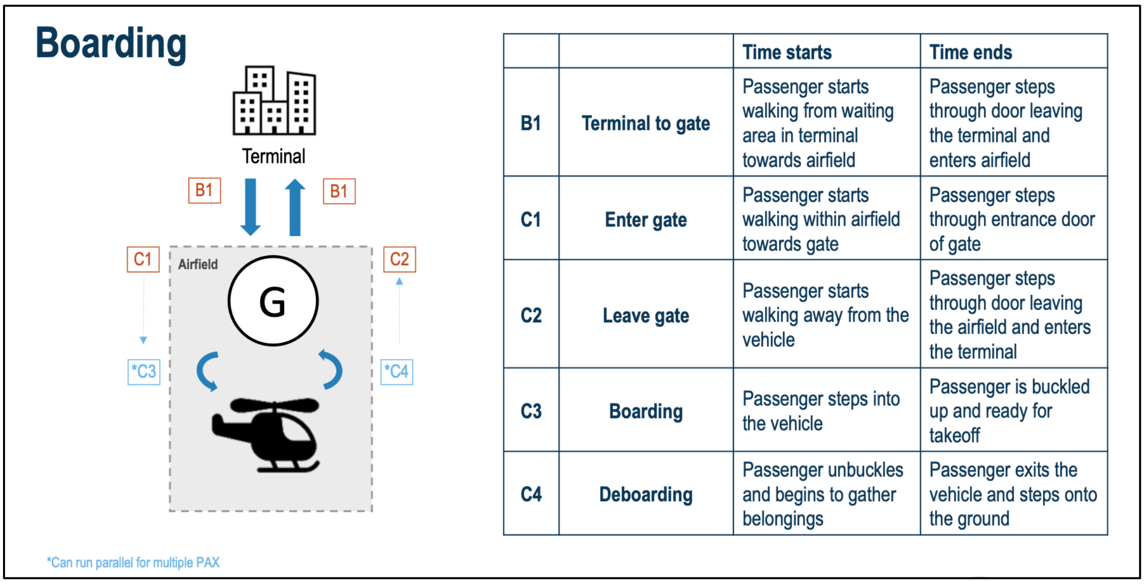

Boarding

		Time starts	Time ends
B1	Terminal to gate	Passenger starts walking from waiting area in terminal towards airfield	Passenger steps through door leaving the terminal and enters airfield
C1	Enter gate	Passenger starts walking within airfield towards gate	Passenger steps through entrance door of gate
C2	Leave gate	Passenger starts walking away from the vehicle	Passenger steps through door leaving the airfield and enters the terminal
C3	Boarding	Passenger steps into the vehicle	Passenger is buckled up and ready for takeoff
C4	Deboarding	Passenger unbuckles and begins to gather belongings	Passenger exits the vehicle and steps onto the ground

*Can run parallel for multiple PAX

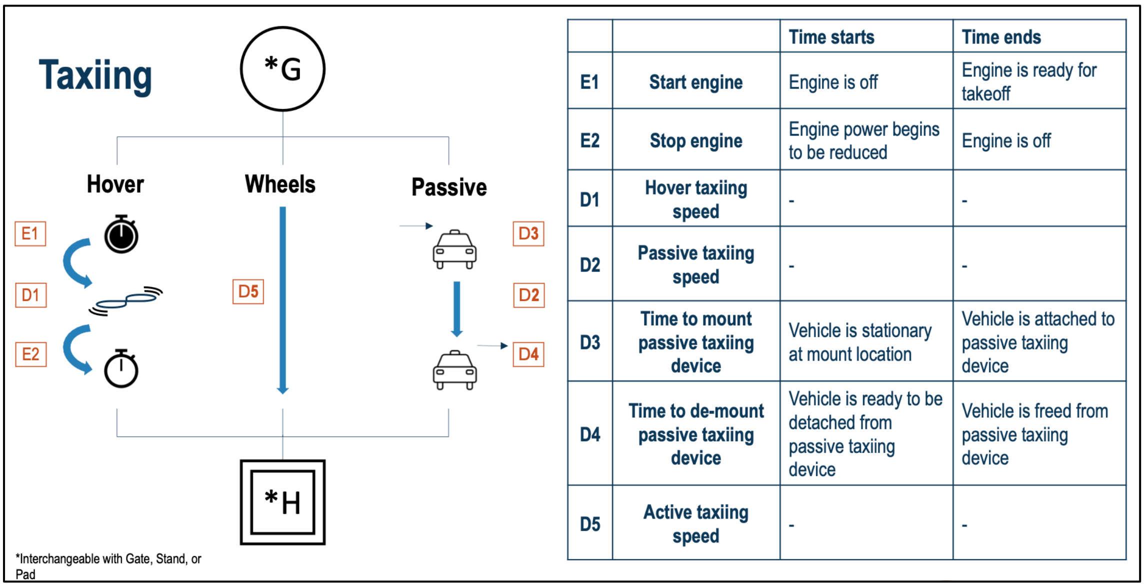

Taxiing

		Time starts	Time ends
E1	Start engine	Engine is off	Engine is ready for takeoff
E2	Stop engine	Engine power begins to be reduced	Engine is off
D1	Hover taxiing speed	-	-
D2	Passive taxiing speed	-	-
D3	Time to mount passive taxiing device	Vehicle is stationary at mount location	Vehicle is attached to passive taxiing device
D4	Time to de-mount passive taxiing device	Vehicle is ready to be detached from passive taxiing device	Vehicle is freed from passive taxiing device
D5	Active taxiing speed	-	-

*Interchangeable with Gate, Stand, or Pad

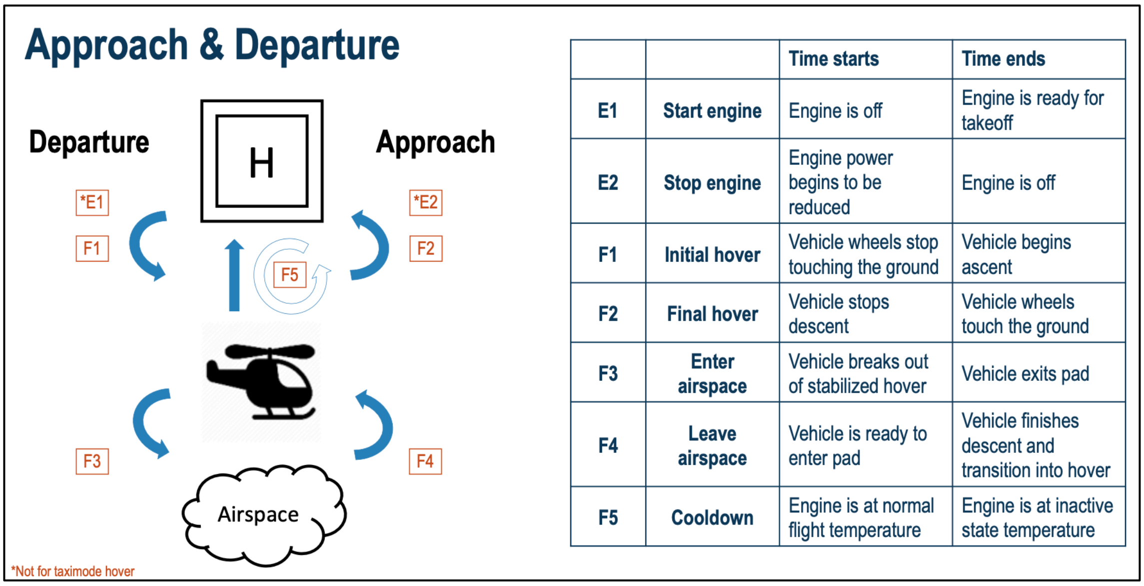

Approach & Departure

		Time starts	Time ends
E1	Start engine	Engine is off	Engine is ready for takeoff
E2	Stop engine	Engine power begins to be reduced	Engine is off
F1	Initial hover	Vehicle wheels stop touching the ground	Vehicle begins ascent
F2	Final hover	Vehicle stops descent	Vehicle wheels touch the ground
F3	Enter airspace	Vehicle breaks out of stabilized hover	Vehicle exits pad
F4	Leave airspace	Vehicle is ready to enter pad	Vehicle finishes descent and transition into hover
F5	Cooldown	Engine is at normal flight temperature	Engine is at inactive state temperature

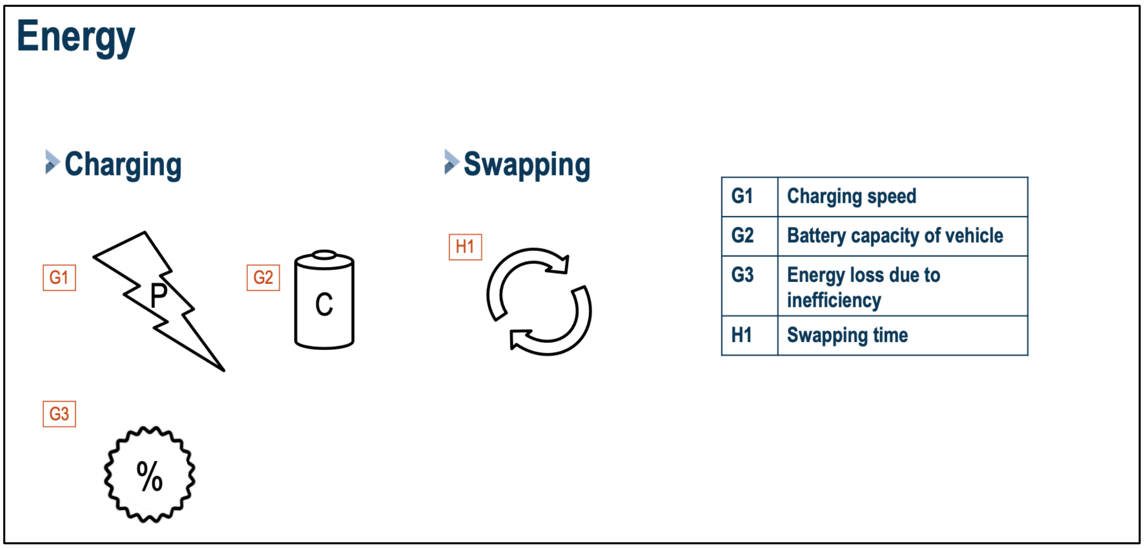

Energy

G1	Charging speed
G2	Battery capacity of vehicle
G3	Energy loss due to inefficiency
H1	Swapping time

Appendix 2: Groups of vertiport operation parameters presented to experts during interview.

Attached to appendix 3 are selected slides from the sneak peek of results that were presented to all 17 experts who participated in the interview series.

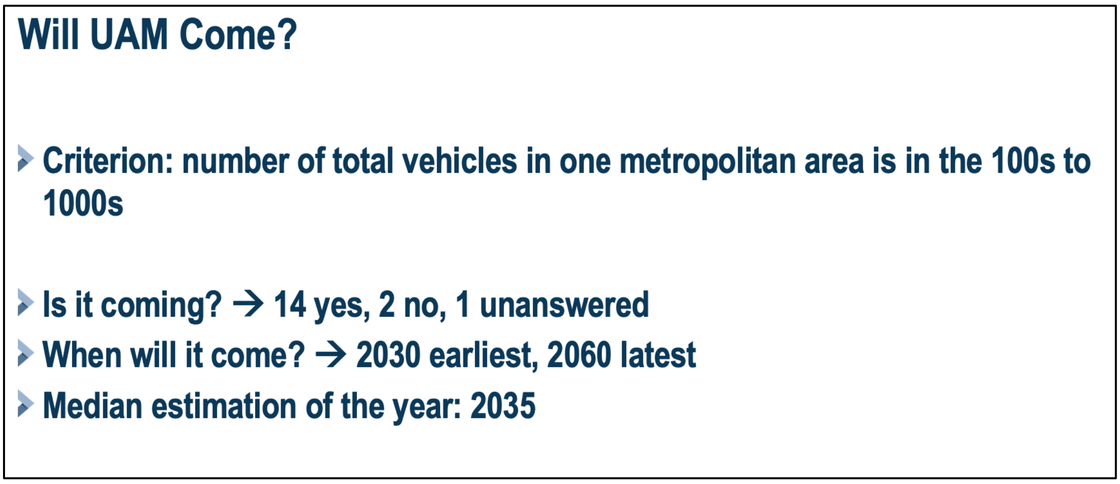

Will UAM Come?

- Criterion: number of total vehicles in one metropolitan area is in the 100s to 1000s

- Is it coming? → 14 yes, 2 no, 1 unanswered
- When will it come? → 2030 earliest, 2060 latest
- Median estimation of the year: 2035

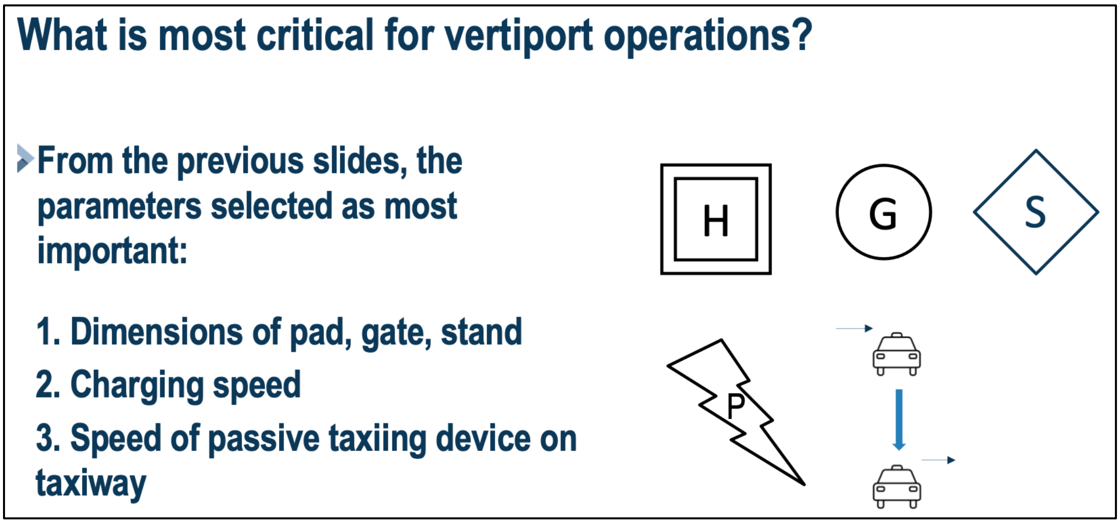

What is most critical for vertiport operations?

- From the previous slides, the parameters selected as most important:

1. Dimensions of pad, gate, stand
2. Charging speed
3. Speed of passive taxiing device on taxiway

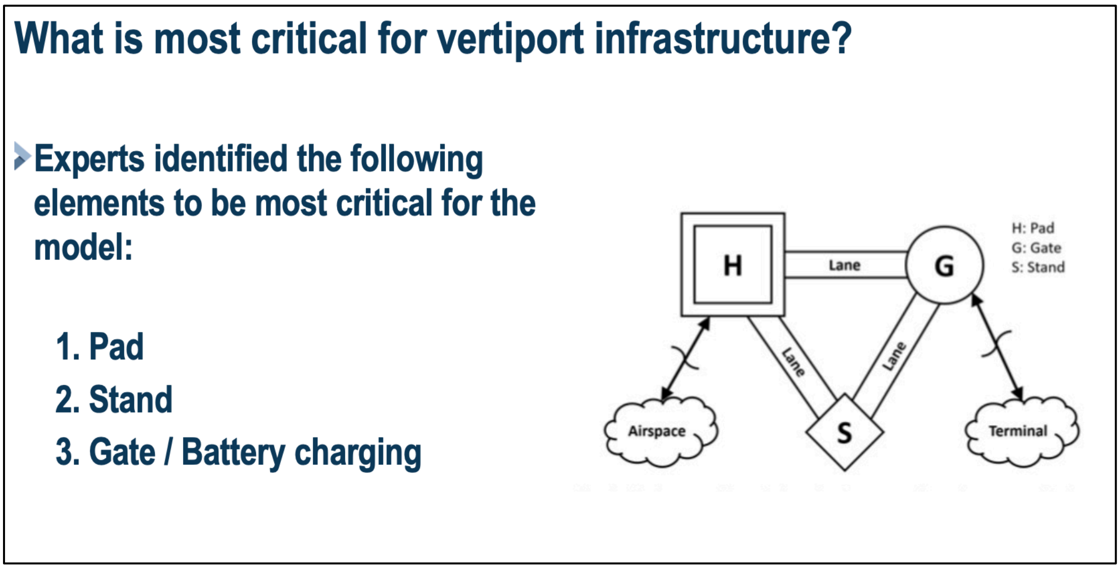

What is most critical for vertiport infrastructure?

- Experts identified the following elements to be most critical for the model:

1. Pad
2. Stand
3. Gate / Battery charging

Appendix 3: Selected slides from sneak peek for expert interview participants.

Appendix 4 contains an example of the elimination process of parameters referenced in section 3.2 “parameter determination.”

ID	Parameter	Comment	Final Action
C9	Safety instruction of passenger	Takes up time before departure	Aggregate with boarding
C11	Store Luggage	Takes up time before departure	Aggregate with boarding
	General Safety Check	Takes up time before departure	Aggregate with boarding
C12	Unloading luggage	Takes up time after landing	Aggregate with deboarding
F11	Cooldown	The emphasis is the time it takes for the physical airspace to be available, pick a name closer to that meaning	Renamed to A/C Separation
H2	Number of standards	If does not affect vertiport operations, discard	Discard
I7	Routine vehicle maintenance necessary after number of flight	If not critical, discard	Discard
J3	Number of operations before cleaning taxiway is necessary	If not critical, discard	Discard
J4	Number of operations before cleaning pad is necessary	If not critical, discard	Discard

Appendix 4: Comparison of parameter versions.

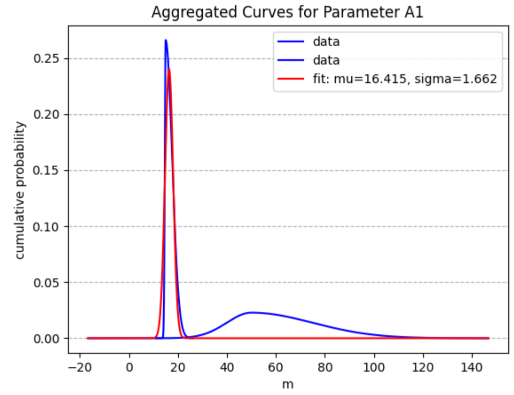
Aggregated Curves for Parameter A1
data
data
fit: mu=16.415, sigma=1.662
cumulative probability
0.00
0.05
0.10
0.15
0.20
0.25
−20
0
20
40
60
80
100
120
140
m

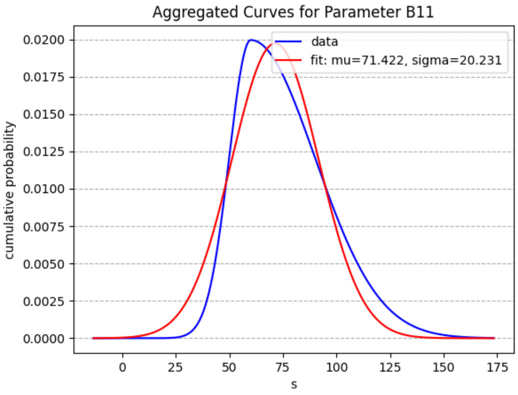
Aggregated Curves for Parameter B11
data
fit: mu=71.422, sigma=20.231
cumulative probability
0.0000
0.0025
0.0050
0.0075
0.0100
0.0125
0.0150
0.0175
0.0200
0
25
50
75
100
125
150
175
s

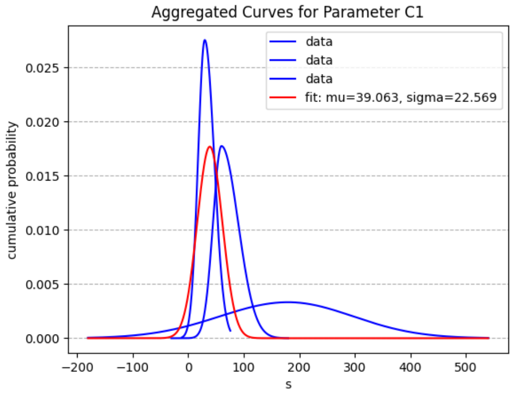
Aggregated Curves for Parameter C1
data
data
data
fit: mu=39.063, sigma=22.569
cumulative probability
0.000
0.005
0.010
0.015
0.020
0.025
−200
−100
0
100
200
300
400
500
s

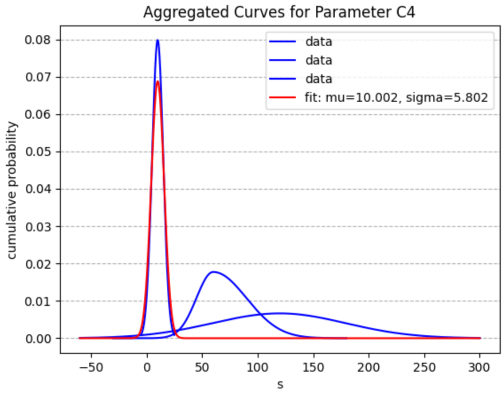
Aggregated Curves for Parameter C4
data
data
data
fit: mu=10.002, sigma=5.802
cumulative probability
0.00
0.01
0.02
0.03
0.04
0.05
0.06
0.07
0.08
−50
0
50
100
150
200
250
300
s

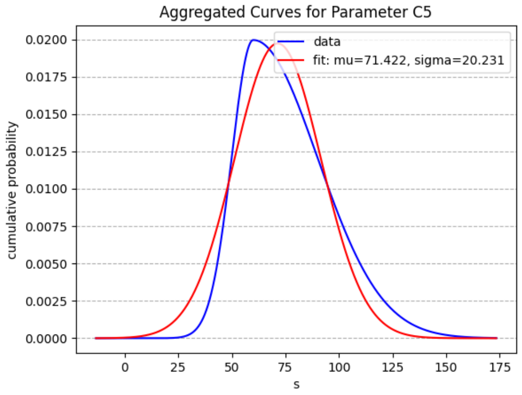
Aggregated Curves for Parameter C5
data
fit: mu=71.422, sigma=20.231
cumulative probability
0.0000
0.0025
0.0050
0.0075
0.0100
0.0125
0.0150
0.0175
0.0200
0
25
50
75
100
125
150
175
s

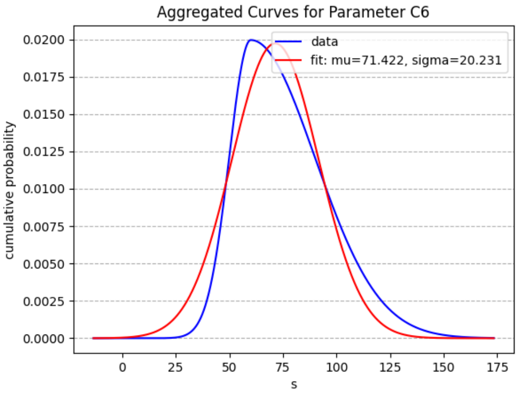
Aggregated Curves for Parameter C6
data
fit: mu=71.422, sigma=20.231
cumulative probability
0.0000
0.0025
0.0050
0.0075
0.0100
0.0125
0.0150
0.0175
0.0200
0
25
50
75
100
125
150
175
s

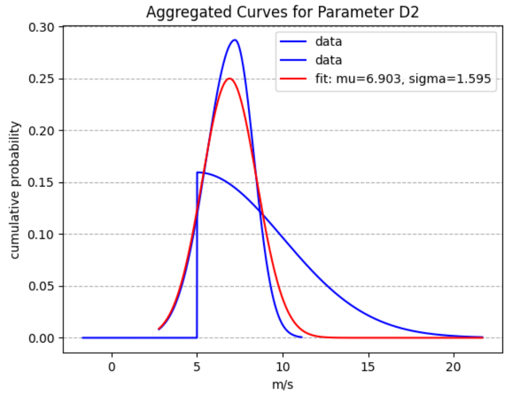
Aggregated Curves for Parameter D2
data
data
fit: mu=6.903, sigma=1.595
cumulative probability
0.00
0.05
0.10
0.15
0.20
0.25
0.30
0
5
10
15
20
m/s

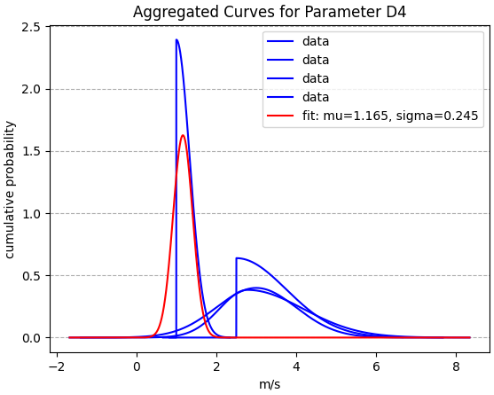
Aggregated Curves for Parameter D4
data
data
data
data
fit: mu=1.165, sigma=0.245
cumulative probability
0.0
0.5
1.0
1.5
2.0
2.5
−2
0
2
4
6
8
m/s

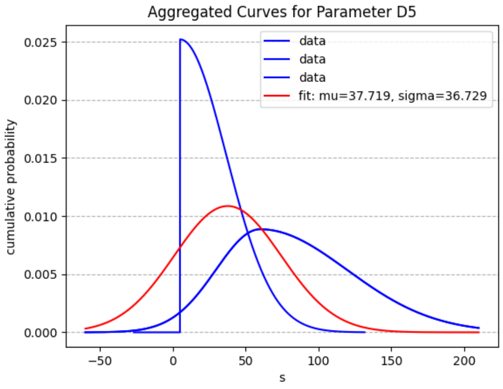
Aggregated Curves for Parameter D5
data
data
data
fit: mu=37.719, sigma=36.729
cumulative probability
0.000
0.005
0.010
0.015
0.020
0.025
−50
0
50
100
150
200
s

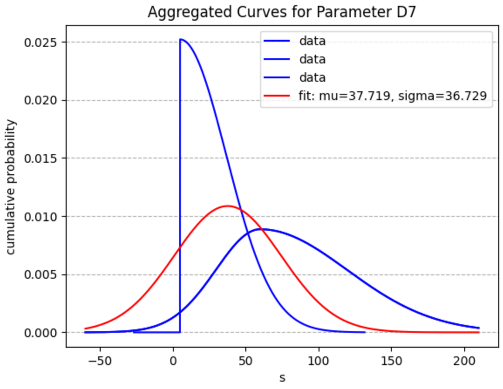
Aggregated Curves for Parameter D7
data
data
data
fit: mu=37.719, sigma=36.729
cumulative probability
0.000
0.005
0.010
0.015
0.020
0.025
−50
0
50
100
150
200
s

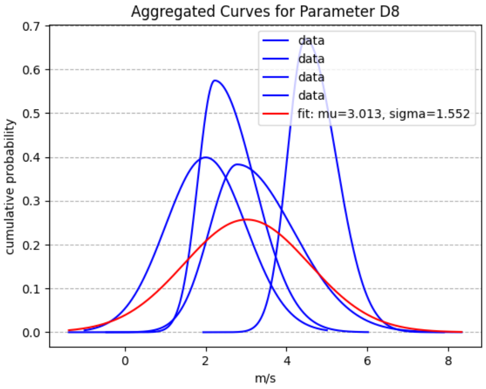
Aggregated Curves for Parameter D8
data
data
data
data
fit: mu=3.013, sigma=1.552
cumulative probability
0.0
0.1
0.2
0.3
0.4
0.5
0.6
0.7
0
2
4
6
8
m/s

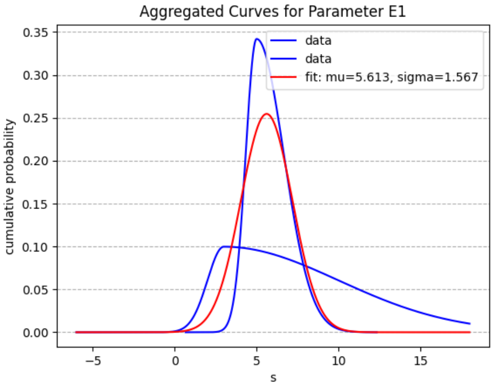
Aggregated Curves for Parameter E1
data
data
fit: mu=5.613, sigma=1.567
cumulative probability
0.00
0.05
0.10
0.15
0.20
0.25
0.30
0.35
−5
0
5
10
15
s

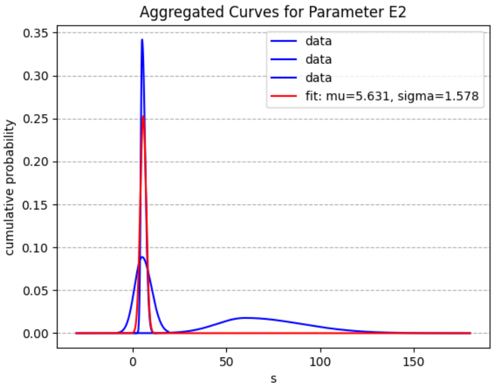
Aggregated Curves for Parameter E2
data
data
data
fit: mu=5.631, sigma=1.578
cumulative probability
0.00
0.05
0.10
0.15
0.20
0.25
0.30
0.35
0
50
100
150
s

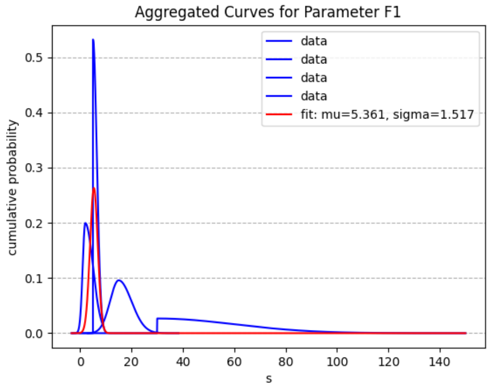
Aggregated Curves for Parameter F1
data
data
data
data
fit: mu=5.361, sigma=1.517
cumulative probability
0.0
0.1
0.2
0.3
0.4
0.5
0
20
40
60
80
100
120
140
s

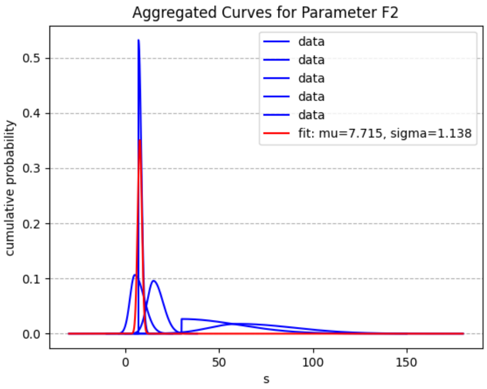
Aggregated Curves for Parameter F2
data
data
data
data
data
fit: mu=7.715, sigma=1.138
cumulative probability
0.0
0.1
0.2
0.3
0.4
0.5
0
50
100
150
s

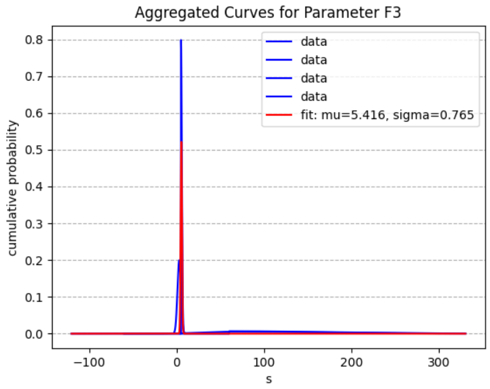
Aggregated Curves for Parameter F3
data
data
data
data
fit: mu=5.416, sigma=0.765
cumulative probability
0.0
0.1
0.2
0.3
0.4
0.5
0.6
0.7
0.8
−100
0
100
200
300
s

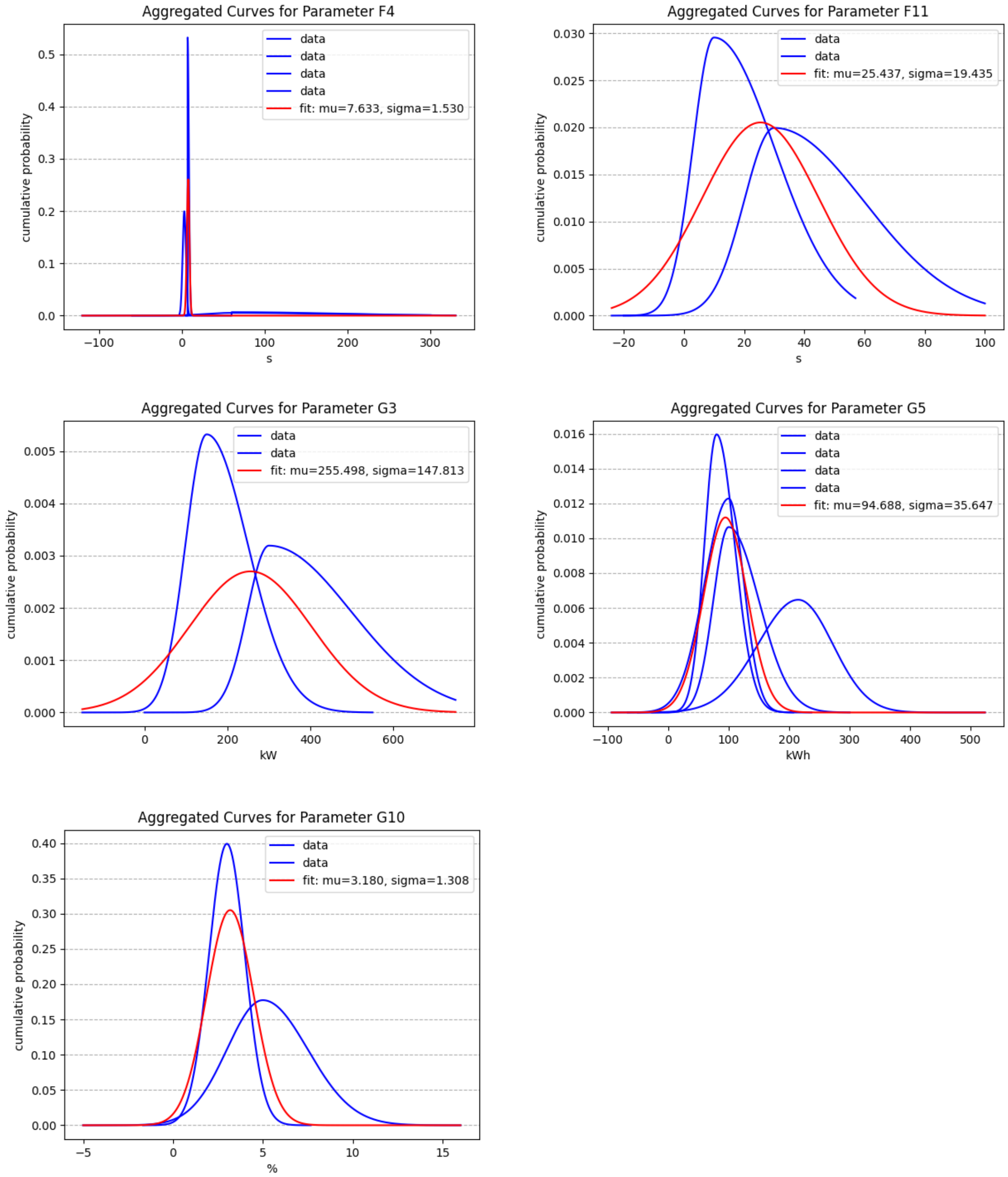

Appendix 5: Skew normal distribution curves (blue) aggregated into normal distribution curves (red) per parameter.